# HyDelta 2

## WP8 – Analysing digitalization in the network management

D8.3 – Simulation results for the selected use cases

D8.4 – Final Report

Status: Final

Dit project is medegefinancierd door TKI Nieuw Gas | Topsector Energie uit de PPS-toeslag onder referentienummer TKI2022-HyDelta.

# Document summary

**Corresponding author**



| **Corresponding author** | Ryvo Octaviano, Demetris Palochis, Jonah Poort, Huib Blokland |
|---|---|
| **Affiliation** | TNO |
| **Email address** | ryvo.octaviano@tno.nl, huib.blokland@tno.nl, jonah.poort@tno.nl, demetris.palochis@tno.nl |



**Document history**

| Version | Date | Author | Affiliation | Summary of main changes |
|---|---|---|---|---|
| 1 | 31-Jan-2023 | Ryvo Octaviano et al. | TNO | Working progress |
| 2 | 19-Apr-2023 | Ryvo Octaviano et al. | TNO | 1st Draft, to be reviewed by EAG |
| 3 | 2-May-2023 | Ryvo Octaviano et al. | TNO | Final draft |
| 4 | 17-May-23 | Ryvo Octaviano et al. | TNO | Final |

**Dissemination level**

| | | |
|---|---|---|
| **PU** | Public | X |
| **RE** | Restricted to<br>• Project partners including Expert Assessment Group<br>• External entity with whom a Non-Disclosure Agreement exists | |

**Document review**

| Partner | Name |
|---|---|
| Stedin | Iman Pishbin |
| Alliander | Reon Baars |
| Enexis | Ruud Busscher |
| Netbeheer Nederland | Stefanie van Kleef |
| NBNL, Gasunie, Kiwa, DNV, TNO, NEC, NDG, OGH2 | HyDelta Supervisory Group |

# Executive summary

Replacing natural gas by hydrogen in the existing DSO infrastructure will give several challenges on the security of supply of energy to the end-users, related to the physical aspects of the assets in the hydrogen network. Within the HyDelta2 program, WP8 Digitalization, the need and benefit of digitalization of the gas grid has been investigated.

In the current gas grid the digitalization is limited in all aspects: monitoring, modelling and control. This means that a lot of digitalization aspects could be developed to handle the needs of a future hydrogen grid, which have to deal with the following trends: increasing dynamics in supply and demand, from a stand-alone grid to a multi-connected grid and a need for real-time data on supply and demand. A roadmap has been developed on how to deal with the main challenges in balancing the future hydrogen grid, for all aspects of digitalization.

In the frame of the HyDelta2 program we have chosen for the use case 'Smart sensor placement' for pressure and flow sensors in the Kapelle area, which covers the main digitalization aspects, with a focus on the short- and mid-term.

On this grid several scenarios have been applied, using TNO's dynamic gas grid simulation tool Aurora. Starting with a base case where natural gas is replaced by hydrogen. Subsequently scenarios have been simulated on adding new supply locations for electrolyzers with a dynamic profile, adding large consumers and a scenario with one 'broken gas pipe'.

The flow and pressure in the whole grid has been simulated for all scenario's, with realistic supply and demand data. The gas grid simulator has been validated in the current (natural gas) situation by available pressure and flow data. By replacing the natural gas by hydrogen and maintaining the delivery of the same amount of energy to all users, the flows in the grid are about three times higher and the pressures will remain about the same. However, the flows stay below the allowable limits. In the case of adding two realistic electrolyzers with a total capacity of 3 MW, the maximum pressures stay below the allowable limits. A N-1 situation has been simulated by a pipe break in the 4 bar grid, showing the critical pipe segments where the pressure becomes too low. In the next scenario three additional large consumers are added, resulting in a pressure drop which is on some locations just below the allowable limit. Finally the effect of replacing the two current supply's by one supply on another location in the grid, has been investigated. The simulation tool has been used to find the optimal locations in terms of pressures and flows within the acceptable limits.

In all scenario's an uncertainty in the domestic demand have been introduced and the number of (flow and pressure) sensors and their location have been determined, to minimize the uncertainty in flow and pressure in the whole grid. The overall picture for the scenario's is that adding two sensors will give the main gain in reducing the uncertainty. Adding two pressure sensors reduces the uncertainty in pressure with about 60% to 70%. Adding flow sensors have a much smaller effect on the reduction due to restriction on placing the sensor. The location for placing the sensor is globally the same for all scenario's.

The different scenario's show the need for a dynamic modelling tool that is able to calculate flows and pressures in the grid in case of a dynamic supply and demand situation. Only a tool will not be sufficient to get full insight, because of uncertainties in the input data for the grid. Besides uncertainty in the demand profile, there can be incompleteness of the geometrical information (pipe diameters, pipe roughness, etc.) and pressure settings which deviate from the numbers that are used in the model. So, to get a full insight in the grid, always measurement data will be needed. The benefit of a simulation

tool to investigate the number and location of sensors has been demonstrated, showing that the number of pressure sensors in the grid should be increased.

Furthermore, the insight in the physical behavior of the grid is essential in the future foreseen increase of the number of local decentralized hydrogen suppliers (both from solar/wind and surplus of the electricity grid) and the ability of DSO's to control and manage the pressure in the distribution network.

Overall, we can draw a conclusion on the added value of digitalization of the gas grid. The gas grid is currently facing several broad challenges which can be aided by digital technologies: different heating technologies, declining amount of customers and gas demand, converting of the grid to hydrogen (and biomethane) and decentralized production. Current standard operations such as maintenance planning and security of supply can benefit from digitalization, by allowing the DSO's to make better decisions and proper investments. Digitalisation will create more accurate and real-time insight and a combination of a robust calculation model and online data from a limited number of sensors will generate sufficient insight, moreover digitalisation will facilitate scenario analysis and creates more opportunities for renewable gasses in the gas network.

# Samenvatting

Het vervangen van aardgas door waterstof in de bestaande DSO-infrastructuur zal verschillende uitdagingen met zich meebrengen op het gebied van de energievoorziening aan eindgebruikers, gerelateerd aan de fysische aspecten van de assets in het waterstofnetwerk. Binnen het HyDelta2 programma is in WP8 'Digitalisering' onderzocht wat de noodzaak en voordelen zijn van digitalisering van het gasnetwerk.

In het huidige gasnetwerk is de digitalisering beperkt op alle gebieden: monitoring, modellering en control. Dit betekent dat er veel aspecten van digitalisering ontwikkeld zouden kunnen worden om te voldoen aan de behoeften van een toekomstig waterstofnetwerk, dat moet omgaan met de volgende trends: toenemende dynamiek in aanbod en vraag, van een stand-alone netwerk naar een multi-conneted netwerk en de behoefte aan real-time gegevens over aanbod en vraag. Er is een roadmap ontwikkeld voor het omgaan met de belangrijkste uitdagingen bij het in balans brengen van het toekomstige waterstofnetwerk, voor alle aspecten van digitalisering.

In het kader van het HyDelta2-programma hebben we gekozen voor het gebruiksscenario 'Slimme plaatsing van sensoren' voor druk- en flowsensoren in het gebied Kapelle, dat de belangrijkste aspecten van digitalisering beslaat, met een focus op de korte en middellange termijn.

Op dit netwerk zijn verschillende scenario's toegepast, gebruikmakend van TNO's dynamische gasnet simulator Aurora. Te beginnen met een basisgeval waarin aardgas wordt vervangen door waterstof. Vervolgens zijn scenario's gesimuleerd voor het toevoegen van nieuwe invoedlocaties voor elektrolyzers met een dynamisch profiel, het toevoegen van grote verbruikers en een scenario met één 'gebroken gasleiding'.

De flow en druk in het hele netwerk zijn gesimuleerd voor alle scenario's, met realistische aanbod- en vraaggegevens. De gasnet simulator is gevalideerd in de huidige (aardgas) situatie aan de hand van beschikbare druk- en flowdata. Door het vervangen van aardgas door waterstof en het handhaven van de levering van dezelfde hoeveelheid energie aan alle gebruikers, zijn de flows in het netwerk ongeveer drie keer hoger en blijft de druk ongeveer gelijk. De stromen blijven echter onder de toelaatbare limieten. In het geval van het toevoegen van twee realistische elektrolyzers met een totale capaciteit van 3 MW, blijven de maximale drukken onder de toelaatbare limieten. Een N-1 situatie is gesimuleerd door een leidingbreuk in het 4 bar netwerk, waarbij de kritieke leidingsegmenten worden getoond waar de druk te laag wordt. In het volgende scenario zijn drie extra grote verbruikers toegevoegd, wat resulteert in een drukdaling die op sommige locaties net onder de toelaatbare limiet ligt. Ten slotte is het effect van het vervangen van de twee huidige invoeders door één invoeder op een andere locatie in het netwerk onderzocht. De simulatietool is gebruikt om de optimale locaties te vinden in termen van druk en stroming binnen de aanvaardbare limieten.

In alle scenario's is er een onzekerheid geïntroduceerd in de afname van de kleingebruikers en is het aantal (flow- en druk)sensoren en hun locatie bepaald om de onzekerheid in flow en druk in het hele netwerk te minimaliseren. Het algemene beeld voor de scenario's is dat het toevoegen van twee sensoren de meeste winst oplevert bij het verminderen van de onzekerheid. Het toevoegen van twee druksensoren vermindert de onzekerheid in druk met ongeveer 60% tot 70%. Het toevoegen van flowsensoren heeft een veel kleiner effect op de vermindering. De locatie voor het plaatsen van de sensoren is globaal hetzelfde voor alle scenario's.

De verschillende scenario's tonen de noodzaak van een dynamische simulator dat in staat is om flows en drukken in het netwerk te berekenen in het geval van een dynamische vraag- en aanbodsituatie. Alleen een tool zal niet voldoende zijn om volledig inzicht te krijgen, vanwege onzekerheden in de invoergegevens voor het netwerk. Naast onzekerheid in het vraagprofiel, kan er sprake zijn van onvolledigheid van geometrische informatie (pijpdiameters, pijp ruwheid, enz.) en drukinstellingen die afwijken van de waarden die in het model worden gebruikt. Dus om een volledig inzicht te krijgen in het netwerk, zullen altijd meetgegevens nodig zijn. Het voordeel van een simulatietool om het aantal en de locatie van sensoren te onderzoeken, is aangetoond, waarbij blijkt dat het aantal druksensoren in het netwerk moet worden verhoogd.

Verder is inzicht in het gedrag van het netwerk essentieel voor de verwachte toename van het aantal gedecentraliseerde waterstofleveranciers (zowel van zonne- / windenergie als van overcapaciteit van het elektriciteitsnet) en het vermogen van de DSO's om de druk in het distributienetwerk te regelen en te beheren.

Over het algemeen kunnen we een conclusie trekken over de toegevoegde waarde van digitalisering van het gasnet. Het gasnet staat momenteel voor verschillende brede uitdagingen die kunnen worden geholpen door digitale technologieën: verschillende verwarmingstechnologieën, afnemend aantal klanten en gasvraag, omzetting van het netwerk naar waterstof (en biogas) en gedecentraliseerde productie. Huidige standaardoperaties zoals onderhoudsplanning en leveringszekerheid kunnen profiteren van digitalisering, door de DSO's in staat te stellen betere beslissingen te nemen en passende investeringen te doen. Digitalisering zorgt voor nauwkeuriger en real-time inzicht en een combinatie van een robuust rekenmodel en online data van een beperkt aantal sensoren zorgt voor voldoende inzicht. Bovendien maakt digitalisering scenarioanalyse mogelijk en creëert het meer kansen voor hernieuwbare gassen in het gasnet.

# Table of contents

# Abbreviation List

| Abbreviation | Meaning |
|---|---|
| DN | Nominal Pipe Size in millimetres |
| DS | District station. A pressure reducing station from 4 bar to 100 mbar |
| DSO | Distribution System Operator. The operator of distribution network (low pressure) |
| G1A | Gas profile for connections with a gas meter G6 or smaller and a standard annual consumption of less than 5000 m3 |
| G2C | Gas profile for connections to a standard annual consumption of 170.000 m3 with operating time greater than or equal to 1500 hours |
| G6 | A gas meter for consumption up to 10 $m^3/h$ |
| GTS | Gasunie Transport Services. The Netherlands gas transmission system operator. |
| KNMI | *Koninklijk Nederlands Meteorologisch Instituut*. The Royal Dutch Meteorological Institute |
| LHV | Lower Heating Value or net calorific value. The amount of heat released by combusting a specified quantity and returning the temperature of the combustion products which assumes the latent heat of vaporization of water in the reaction products is not recovered. |
| MPE | Mean Percentage Error. The computed average of percentage errors by which forecasts of a model differ from actual values of the quantity being forecast. |
| MW | Mega Watt is 1 million Watt (the unit of power). |
| NEDU | *Vereniging Nederlandse Energie Data Uitwisseling*. Dutch Energy Data Exchange who provides the gas and electricity standard consumption profile |
| PV | Photovoltaics. The conversion of light into electricity using semiconducting materials |
| SJV | *Standaard Jaarverbruik*. The expected annual consumption of gas on a connection in a standard year |
| STP | Standard temperature and pressure at 288.15 K (15 0C) and 101.325 kPa |
| TNO | *Toegepast-natuurwetenschappelijk Onderzoek*. The Netherlands not-for-profit knowledge organisation |
| TSO | Transmission System Operator. The operator of transmission network (high pressure) |
| XML | Extensible Markup Language. A simple text-based format for representing structured information |

# 1 Introduction

Replacing natural gas by hydrogen in the existing DSO infrastructure will give several challenges (next to safety aspects, social acceptance, etc.) on the security of supply of energy to the end-users, related to the physical aspects of the assets in the hydrogen network. Within the HyDelta2 program, WP8 Digitalization, an analysis is done where digital technology can contribute in accelerating the natural gas grid transformation.

In the first part of the project an investigation has been done on the state of the art of digitalization in the current (natural) gas grids. Furthermore a gap analysis has been performed to define the necessary steps towards a future hydrogen grid, described in a public report [1]. A summary of this investigation is given in the infographic below.

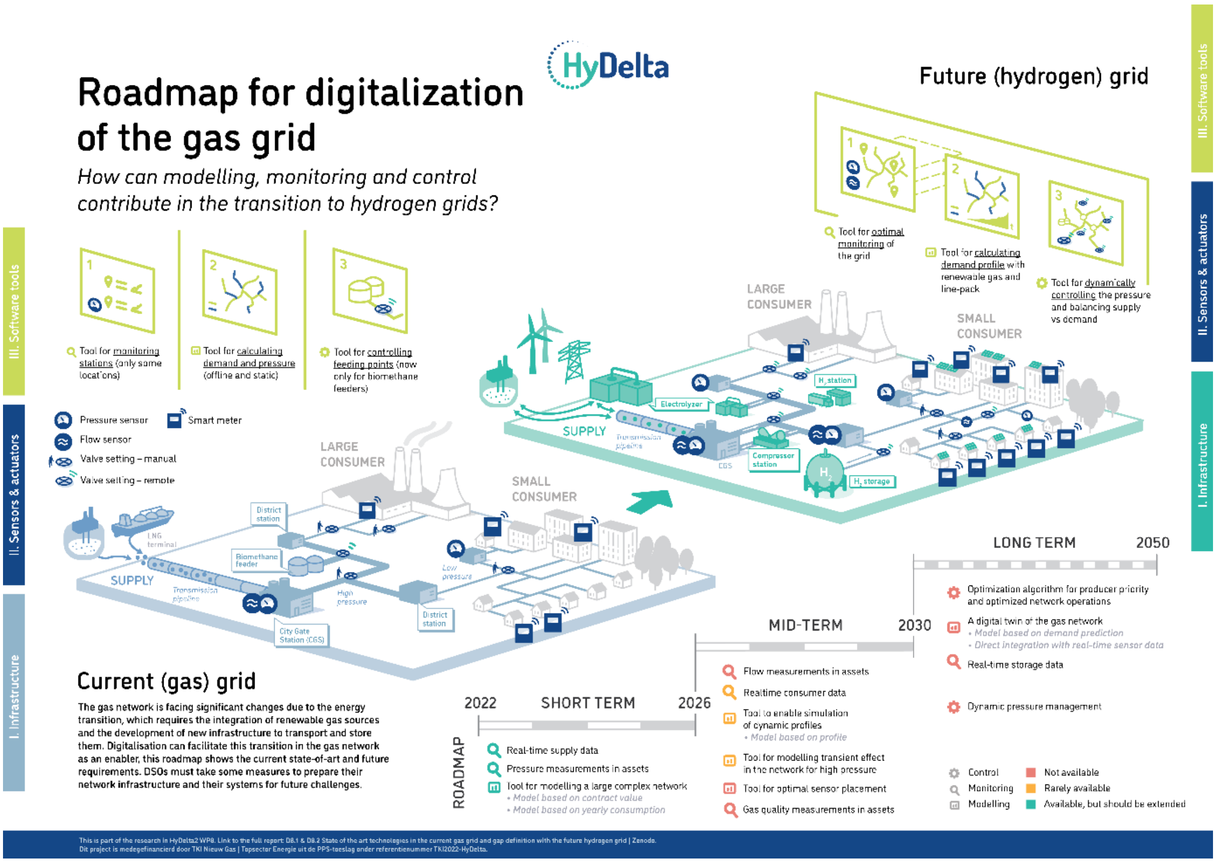


*Figure 1-1 Infographic on the roadmap for digitalization of gas grids*

In the current gas grid the digitalization is limited in all aspects: monitoring, modelling and control. This means that a lot of digitalization aspects could be developed to handle the needs of a future hydrogen grid, which have to deal with the following trends: increasing dynamics in supply and demand, from a stand-alone grid to a multi-connection grid (working together with other DSO, TSO and other energy grids like electricity and heat) and a need for real-time data on supply and demand.

In the above infographic the elements are shown on **how** to deal with the main challenges in balancing the future hydrogen grid, for all aspects of digitalization. In the frame of the work on digitalization in the HyDelta2 program we have chosen for the use case 'Smart sensor placement' which covers the main digitalization aspects, with a focus on the short- and mid-term:

- Use of real-time (local) supply data
- Need and added value of consumer data
- Added value of flow measurement in the grid
- Added value of pressure measurement in the grid
- Tool for a large complex network
- Tool to enable simulation of dynamic supply and demand profiles

In the use case 'Smart sensor placement' the optimal number of flow and pressure sensors and their location will be calculated for a complex grid with both industrial and domestic users to get full insight in the physical behaviour of the grid.

The use case will be performed on a realistic grid: the Kapelle area in Zeeland which full fills all above criteria and on top of that it is also selected by WP7 of the HyDelta2 program. On this grid several scenario's will be applied, starting with a base case where natural gas is replaced by hydrogen. Subsequently scenario's will be simulated on adding new supply locations for electrolyzers with a dynamic profile, adding large consumers and a scenario with one 'broken gas pipe'.

For all these scenario's an uncertainty in the domestic demand will be introduced and the number of (flow and pressure) sensors and their location will be determined, to minimize the uncertainty in flow and pressure in the whole grid.

The report is divided into six chapters. The current chapter describes the introduction and the objective of this report. Then, it is followed by Chapter 2 where the methodology of smart sensor placement is described including the mechanism of the gas grid simulator which is being used to simulate the case. The chosen scenarios and definition are presented in the Chapter 3. The gas grid simulator validation results and smart sensor placement results for pressure and flow sensors are shown in Chapter 4. Chapter 5 explains the observations, findings and conclusions. Finally Chapter 6 will close and summarize and conclude the total work that has been done in WP8 regarding the need and benefit of digitalization of the gas grid.

# 2 Methodology

## 2.1 Gas Grid Simulation

### 2.1.1 Kapelle gas grid

We choose Kapelle municipality in the province Zeeland as a use case because it is also being used in WP7 of HyDelta2. The gas network in Kapelle is operated by Stedin. The situation in Kapelle is a combination of a residential area and an industrial area. This makes the case unique because it combines elements that are realistic for the near future. Think of the connection to the national hydrogen backbone by GTS and possibilities for local supply through electrolyzers. In addition, it is expected that the industry will apply system integration (Electricity-Gas-Hydrogen) which is also an interesting development.

Kapelle has two gas suppliers. Both gas suppliers have a pressure setpoint output at 4 bar. There are 26 District Stations (DS) that reduce the pressure from 4 bar to 100 mbar. (see Figure 2-1Figure ). The network consists of two pressure levels, 4 bar pipelines (green line) and 100 mbar pipelines (blue line).

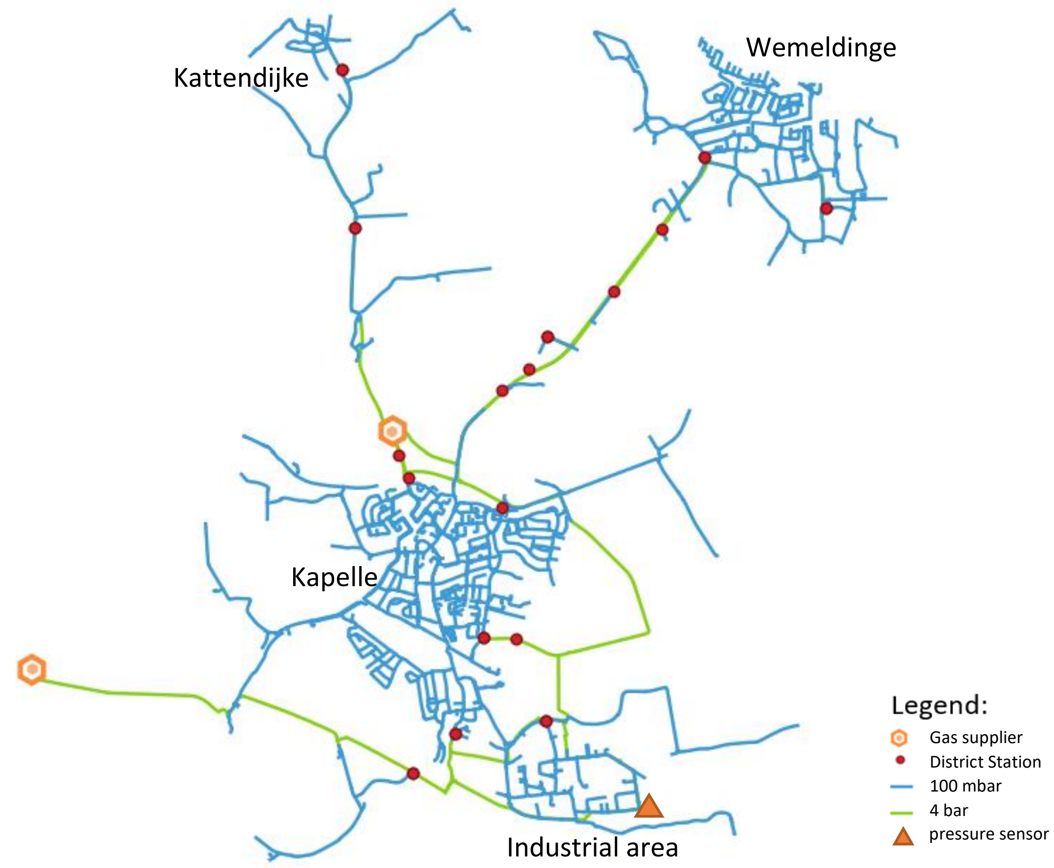


*Figure 2-1 Overview gas network in Kapelle*

Kapelle network consists of three area's (postcode PC4 level): Kapelle, Wemeldinge, and Kattendijke. There are around 5800 small consumers and 17 large consumers in this region. The total natural gas flowrate in the peak demand in winter is around 7000 Nm$^3$/h where 70% of the flow is supplied from gas supplier 1 and 30% is supplied by gas supplier 2. During weekdays, the total large consumers flow is 50-60% and total small consumers flow is 50-40%. While during weekend, the ratio of total large consumers flow and total small consumers flow is 1:9.

During period November 2021 to March 2022, a temporary pressure sensor measurement is placed near large consumer in the Southeast side of the network.

### 2.1.2 Aurora gas simulator

The TNO tool Aurora gas simulator will be used in this work package to simulate and analyze the Kapelle gas grid network transition from natural gas to hydrogen and also for generating data for the optimal sensor placement algorithm.

Aurora [2] is a TNO proprietary solver for computing pressure, flow and composition in a distributed gas grid (low pressure network) and transportation grid (high pressure network). The equation of the pressure drop in pipelines due to friction can be computed from the mass balance and energy balance. This solver can also handle both static (quasi steady-state) and dynamic (transient) behavior of the system. Together with heat network and electricity solver, Aurora gas solver is used in TNO multi-commodity grid tool as seen in Figure 2-2.

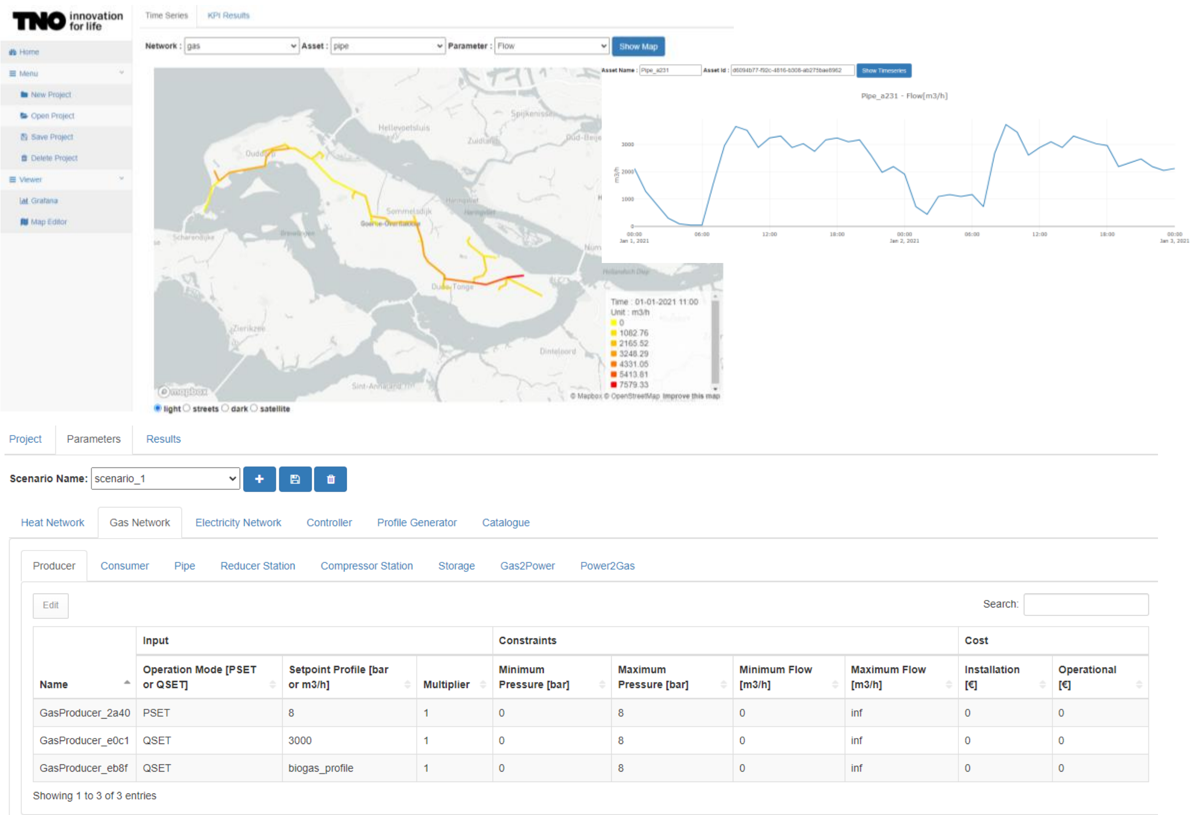


*Figure 2-2 Screenshot of TNO multi-commodity grid tool using Aurora gas pipeline solver*

### 2.1.3 Simulator validation workflow

Validation of the simulator is needed in order to have trusted results for analysis of the hydrogen network and to perform optimal sensor placement workflow. The validation is done on the current natural gas grid situation.

The Kapelle grid itself has two measurements locations: flow and pressure measurement at the gas supplier 1 and one pressure measurement at a 4 bar pipeline in the southeast area close to industrial demand (see Figure 2-1).

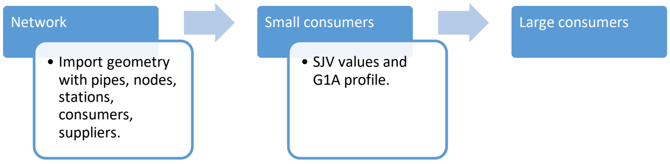


*Figure 2-3 Workflow gas grid validation*

Several steps are taken for the simulator validation of the Kapelle gas grid (Figure 2-3):

1. Network import
   The first step is to import the network information (pipes, stations, consumers, and suppliers) from Kapelle grid into Aurora. The data is exported to XML from Irene Pro software used by Stedin. Since the imported data does not model the individual pipe goes to house for each consumer, thus we add all consumers in the postcode (PC6) level at the end node of pipe in that street.

2. Input profile small consumer
   Since the network operator does not have access to smart meter of small consumer due to privacy reason, thus there is no hourly data consumption available. We use a consumer model to predict the hourly consumption profile based on "*Standard annual consumption*" (SJV), standard gas consumption profile from NEDU (Dutch Energy Data Exchange), and weather data information from the nearest KNMI weather station (310 Vlissingen). The G1A profile is used for connections with a gas meter G6 or smaller and a standard annual consumption of less than 5000 m3.

3. Input profile large consumer
   The hourly consumption profile for the large consumer which have a consumption of more than 170 $m^3/h$ is available. However, other large consumers data are not available. Thus we use a similar approach like the small consumer but now using the G2C profile for the other connections with a standard annual consumption of up to 170,000 m3 of natural gas. We have the SJV value of each large consumer.

4. Boundary conditions
   The station is operated by pressure setpoint. The pressure boundary condition for the gas supplier 1 station is set from the pressure measurement data which is around 4 bar. Since there is no pressure data at the gas supplier 2, we use there 4 bar as the pressure setpoint.

5. Simulation period
   The simulation is run from 21 November 2021 to 31 December 2021 with an hourly timestep. This period is chosen due to availability of temporary pressure measurement data at the large consumer near Southeast industrial area.

### 2.1.4 Simulator validation with measurement data

Before the grid will be used for hydrogen and the several scenario's, the simulation tool will be validated on the current situation and the available data. All based on natural gas. The validation workflow has been describe in the Section 2.1.3.

There are two locations where measurement data is available, as seen in Figure 2-4. At the gas supplier 1 station, we have both pressure and flow measurements and at the southeast, we have a pressure measurement. There is no pressure and flow measurement at the gas supplier 2.

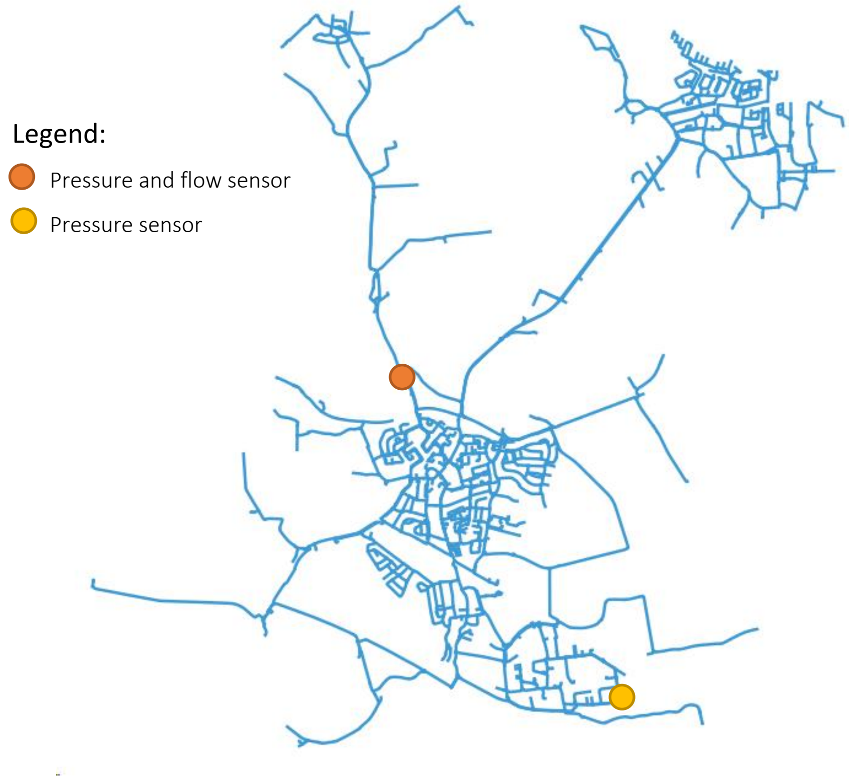


*Figure 2-4 Location of measurement sensors in the Kapelle gas grid*

After running the simulation for the period 22-11-2021 to 31-12-2021, we have simulation results which can be compared with measurement data, as presented below:

1. <u>Comparison flow measurement at the gas supplier 1</u>
   Due to privacy for the timeseries flowrate data, we normalized the flowrate data in presenting the result. The error in timeseries between measured flowrate and calculated flowrate at the gas supplier 1 is shown in Figure 2-5. The gas supplier 1 flow is calculated using simulation results based on a pressure distribution in the network, with a fixed pressure setpoint of gas supplier 1 and gas supplier 2. The total flowrate is calculated from the total flowrate of small consumers and large consumers. The Mean Percentage Error (MPE) of calculated flowrate and measured flowrate at gas supplier 1 is 8.81%. However, the calculated flowrate capture the dynamic behavior quite well. If we have flow and pressure measurement at gas supplier 2, the amplitude difference can be further improved.

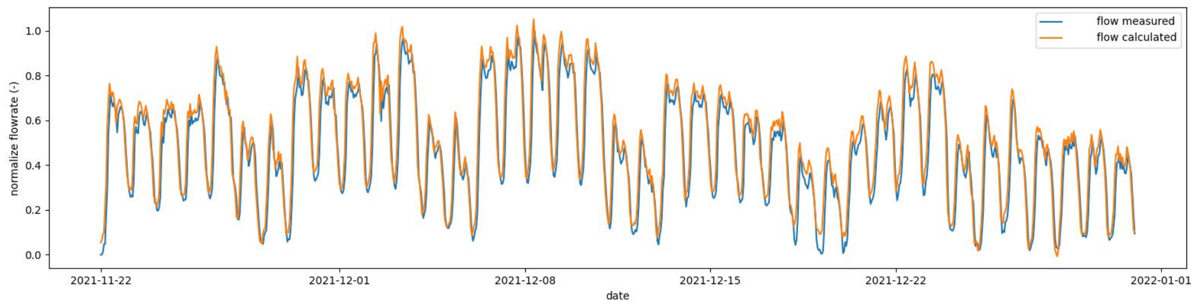


*Figure 2-5 Comparison between normalized measured and calculated flow at the gas supplier 1*

2. <u>Comparison pressure measurement at the southeast</u>
   The error in timeseries between measured pressure and calculated pressure at the Southeast location is shown in the Figure 2-6. The Mean Percentage Error (MPE) of pressure between model and measurement is 0.7%. As can be seen in Figure 2-6, the calculated pressure lies in between upper and lower bound limit of pressure measurement sensor.

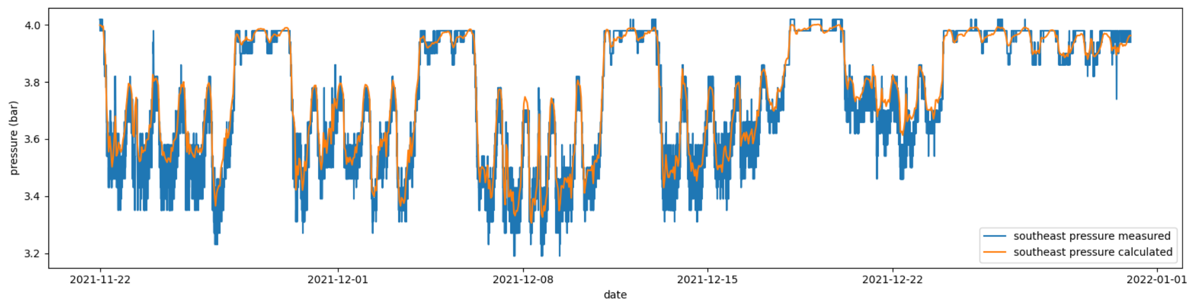


*Figure 2-6 Comparison between measured and calculated pressure at the southeast*

From the comparison above, we have confidence in using Aurora for the simulations in analyzing the Kapelle grid. The total flow at the injection point of natural gas is accurately predicted by the simulator from the hourly demand profile of small consumers and hourly demand profile of large consumers. The pressure at the southeast, where it is the lowest pressure (or the biggest pressure drop) in the 4 bar network due to connected to industrial area, is also accurately predicted by the simulator.

### 2.1.5 Line pack storage in the Kapelle

The imbalance between supply and demand due to intermittent production can be tackled by using storage or line pack. However the line pack in the distribution network will not be as big as line pack in the transmission network of TSO's hydrogen backbone, but it is still worthwhile to quantify the flexibility of the network. In this case, we evaluate the line pack capacity at the 4 bar grid in Kapelle. As discussed with the DSO, it is possible to have a pressure swing between 3 to 5 bar in the 4 bar pipeline. The analytical formula to determine the line pack in a pipeline system is taken from [3].

$$V_{storage} = V_{geometric}\left[\frac{p_m}{Z_m} - \frac{p_m'}{Z_m'}\right] \cdot \frac{1}{p_n}\frac{T_n}{T}$$

Where,

$V_{storage}, V_{geometric}$ are the linepack and the geometric volume of the pipe in $Nm^3$ and $m^3$
$p_m,\ p_m'$ are the upper and lower mean pressure in bar

$Z_m$, $Z_m^{'}$ are the respective compressibility factors
$p_n$, $T_n$ are pressures in bar and temperature in Kelvin at normal conditions

For the 4 bar pipeline, the $V_{geometric}$ is 381 m$^3$. The $p_m$ is 5 bar and the $p_m^{'}$ is 3 bar. The $Z_m$ is 1.0036 and the $Z_m^{'}$ is 1.0024. T is 288.15 K. Thus the line pack volume is 709 Nm$^3$

Assuming the 1 MW electrolyzer has a maximum hydrogen flow of 250 Nm$^3$/h, the line pack is equivalent with ~3 hours of no production (imbalance). This line pack can be utilized for summer demand (200-700 Nm$^3$/h), but not for winter demand where the peak demand is around 21000 Nm$^3$/h.

## 2.2 Optimal Sensor Placement

In this section, an overview is given of the method developed for optimizing the placement of sensors in gas grids. The first subsection introduces the topic and explains the basic workflow that was created, the following subsection details how the general workflow differs between pressure and flowrate sensors specifically.

### 2.2.1 Workflow description

When modelling the state of the flows in a gas grid, the simulation software gives the demand at each consumer in the grid, and calculates the corresponding pressures and flowrates in the network that satisfy these demands. When the demands at the consumers are exactly known, the simulation software can very accurately determine the state of the system, and, depending on model accuracy, no sensors might be needed in the grid.

However, in reality the actual consumption at each consumer is not exactly known, and differs from consumer to consumer, day to day, based on many different factors. For instance, one person might turn down their heating and leave for work around 8:30, while another does so already at 7:30. Other days, someone that normally leaves for work at 9:00 instead works from home and leaves the heating on the entire day.

As a result, the actual state of the grid will always differ from what is modelled based on expected consumption profiles. By placing sensors in the grid, it is possible to measure the real state and update our estimates based on these measurements. Ideally, we would have sensors at every pipe, or at least at every consumer, but in reality this will be prohibitively expensive to do, often infeasible, and could clash with privacy concerns. Therefore, we want to find the optimal locations in the grid to place sensors, such that the model estimate of all flows/pressures in the network can be improved the most with the fewest number of sensors.

The developed sensor placement optimization method is based on work done in [4]. The method starts with a base demand at each consumer, and then runs a large number of Monte Carlo simulations in which each demand is randomly changed for every individual simulation, mimicking the randomness that would be seen in the real world demand as described previously. Monte Carlo approach is chosen because it provides multiple possible outcomes based on the probability compared to deterministic approach. This results in a large set of flow/pressure simulation results, which give an estimate of the grid's state with a corresponding uncertainty in each pipe/node (the standard deviation of the model variations). This is visually shown using a simplified fictional example in Figure 2-7.

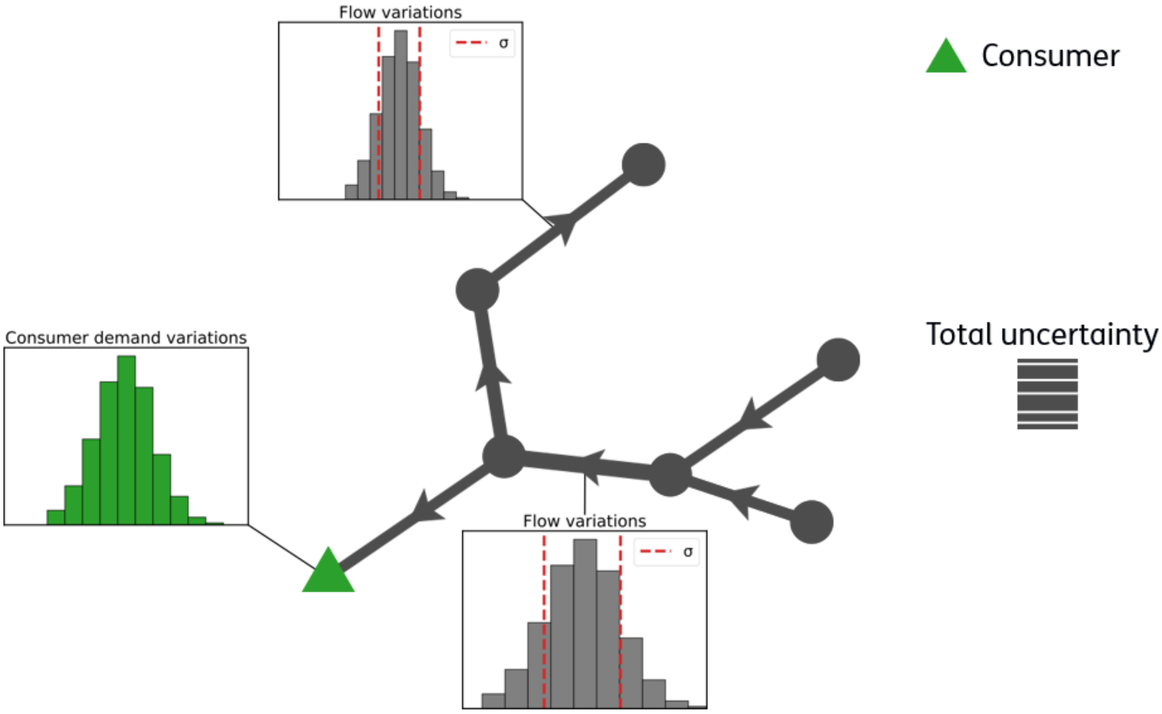


*Figure 2-7 Fictional example of parts of a network containing a single consumer with varying demand, and two examples of the resulting variations in flowrates. The width of each pipe indicates the uncertainty (standard deviation) of these variations. The goal of the sensor placement optimization method is to find the location(s) to put a sensor in such that the total uncertainty of all pipes combined is minimized*

Once the initial model estimate of the uncertainty in the network is known, the sensor optimization algorithm can be executed. The method uses a greedy optimization scheme that places sensors one by one, each time the algorithm evaluates all possible locations, finds the current best location and puts a sensor there, then reevaluates all remaining location for the second best location, etc.

In technical terms, the objective function of our algorithm is the total uncertainty (standard deviation) of flow/pressure in all pipes/nodes the entire network summed up. By placing sensors in the grid, we can reduce this uncertainty. The ultimate goal is to find the locations in the network where placing a sensor reduces the total uncertainty the most (i.e. we aim to minimize the total uncertainty by putting sensors in the right locations).

The potential improvement a sensor gives in our model estimate is two-fold (see Figure 2-8): the first improvement comes from the fact that when a sensor is placed in a pipe/node, the corresponding uncertainty in that pipe/node is removed (Figure 2-8a), as now there is a direct measurement in the pipe/node[1]. The second improvement comes from the fact that now that we know the flow/pressure in one pipe/node, we can update our estimate of all neighboring flows/pressures, further reducing the total uncertainty in the network (Figure 2-8b).

[1] In reality the uncertainty is not removed completely as the sensor itself also has its own measurement error. However, as this error is typically much lower than the modelled uncertainty, in practice is comes down to removing the uncertainty almost entirely.

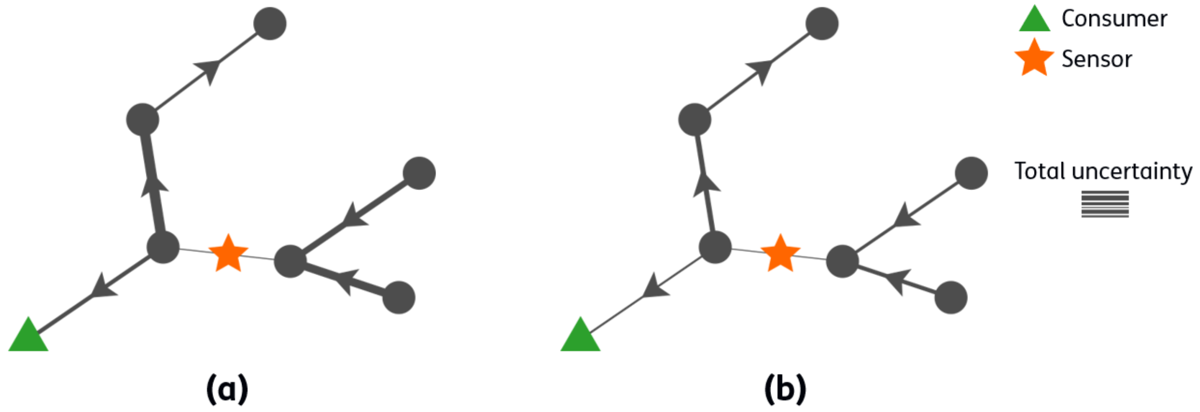


*Figure 2-8 Fictional example showing the two ways in which placing a sensor reduces the uncertainty in a network. First, the uncertainty in the pipe/node the sensor is placed in reduces almost entirely (a), and secondly, using the now known flow in the sensor pipe, the flowrate estimate of surrounding pipes can also be improved (b).*

While the first improvement is straightforward to determine, the second improvement is a bit more involved. It makes use of the large set of Monte Carlo simulation results to make a new estimate of the standard deviation in each pipe in the network by calculating the variance (square of standard deviation) in the pipe through the mass balance or pressure drop between the location of this pipe and location of the sensor.

### 2.2.2 Flowrate sensor placement

This process is most easily explained using an example. Figure 2-9 shows a part of a branch in an example grid with a sensor placed in pipe A (orange star). The aim is to estimate the flow uncertainty in the blue pipe I. This is done by first setting up the mass balance that calculates the flowrate in I based on the incoming and outgoing flowrates in all other pipes between the sensor and the blue pipe (red pipes and sensor pipe A). By doing so, the following sum is found:

$$Q_I = Q_A - Q_B - Q_C - Q_E + Q_G - Q_H$$

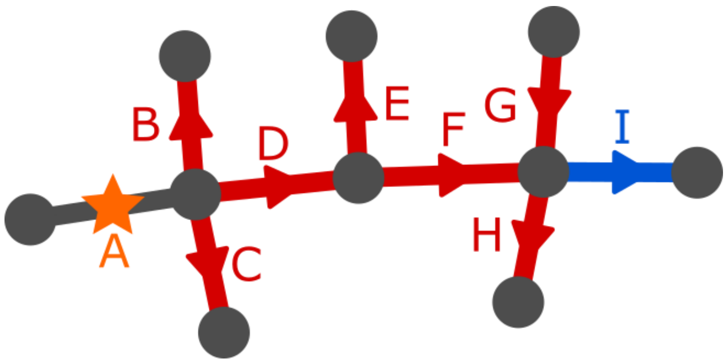


*Figure 2-9 Example of part of a larger gas grid used to explain flow uncertainty estimation through variance calculations. The flow variance is estimated at the blue pipe I, while a sensor is located in pipe A*

In order to estimate the uncertainty reduction achieved by placing a sensor in a given pipe/node, the above calculation is repeated for every pipe in the network. Thus, if a grid contains 1000 pipes, the process is repeated for every one of these 1000 pipes, and the results are summed together to get the new estimate of the total uncertainty in the network. To find the optimal sensor location, this process is repeated for every location in which a sensor can be placed, and the sensor is placed in the pipe where the resulting total uncertainty is the smallest out of all possible locations.

However for the Kapelle network, we can't put sensor in any random pipe due to restriction in implementation. Thus the location for placing flow sensor is limited to at the station only.

### 2.2.3 Pressure sensor placement

The pressure sensor placement algorithm uses the pressure drop in the pipes to make an estimate of the pressure in a node. This pressure calculation is shown in Figure 2-10, using the same example grid part as Figure 2-9. By starting with the pressure in the node containing the sensor (node 1), an estimate can be made for the pressure in the blue node 2 by adding the pressure drops over pipes A, D, and F[2]. This results in the following sum:

$$P_2 = P_1 - \Delta P_A - \Delta P_D - \Delta P_F$$

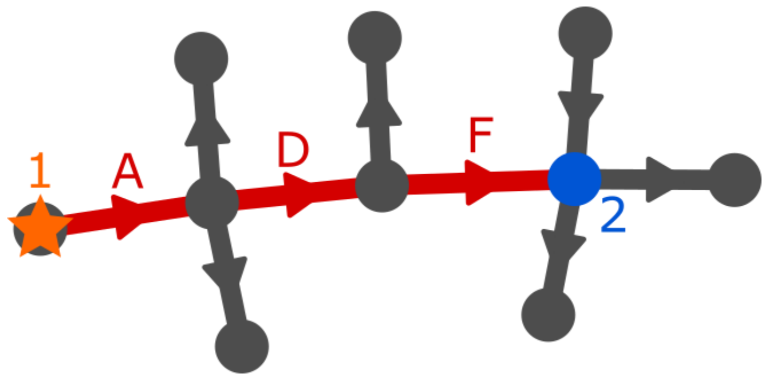


*Figure 2-10 Example of the same part of a larger gas grid as in Figure 2-9, now used to explain pressure uncertainty estimation through variance calculations. The pressure variance is estimated at the blue node 2, while a sensor is located in node 1*

While the pressure estimation method in principle doesn't vary a lot from the flowrate estimation method, it does differ in one key aspect, that will be quite clear when discussing the results later in the report. Since the pressure estimate only includes the pressure drops in the pipes directly in between the sensor and node to estimate, while the flowrate estimate includes all branching pipes, the pressure estimate on average includes less terms in its sum. As a result, the covariance estimate of the pressure also includes fewer terms. Since each term in the sum typically adds additional uncertainty, the pressure sensor estimate will in general be better than that for flowrate. For example, while the distance between sensor and pipe/node to evaluate in Figure 2-9 and Figure 2-10 are both equal, the flowrate sum includes six terms, while that for pressure includes four terms. As a result, the total uncertainty decrease will generally be much better for the pressure sensor placement algorithm than for the flow sensor placement algorithm.

[2] If an estimate would be made for an upstream node, the pressure drop would be *subtracted* instead

# 3 Scenario Definition

The use case 'smart sensor placement' will be performed on a realistic grid, i.e. the Kapelle area in Zeeland. On this grid several scenario's will be applied, to cover the high priority topics as investigated in the gap analysis: use of real-time (local) supply data, need and added value of consumer data, added value of flow and pressure measurement in the grid and the need for a dynamic simulation tool which can handle a large complex network with dynamic supply and demand profiles.

The scenarios have been defined will be further explained in the sections below. Starting with a base case where natural gas is replaced by hydrogen. Subsequently scenario's will be simulated on adding new supply locations for electrolyzers with a dynamic profile, adding large consumers and a scenario with one 'broken gas pipe'.

*Table 3-1 List of scenario definition*

| Name | Description |
|---|---|
| Scenario 0 | This is the base scenario for the reference comparison. It uses the existing natural gas infrastructure and the natural gas is converted to hydrogen, both gas properties and gas demand. |
| Scenario 1 | In this scenario, two additional gas suppliers are added. These represent a distributed electrolyzer in the future generated by renewable electricity source (wind turbine or solar farm). |
| Scenario 2 | This scenario evaluates the robustness in the system when there is an event of pipe break e.g. due to maintenance. |
| Scenario 3 | In this scenario, three additional large consumers (industrial) are added. This scenario is used to evaluate the impact in the current infrastructure, whether reinforcement is needed. |

## 3.1 Scenario 0: Base scenario

The existing gas network is currently used for distributing natural gas to the consumers. Scenario 0 aims to investigate what are the effects of switching to hydrogen. This means, in the same pipelines and at the same pressure levels, hydrogen is supplied from the two injection points, gas supplier 1 and gas supplier 2, to the existing consumers with the same energy demand.

To simulate the flow of hydrogen and keep the energy demands constant, some changes are necessary. More specifically, the properties of hydrogen gas are used in the Aurora simulator and the flow demands at all of the consumers were multiplied with a factor of 3, since this factor is approximately the ratio of energy density of natural gas to hydrogen. Above, you can see the calculation of the factor. For energy density, the lower heating value times the density is estimated. Then, the factor is calculated from the ratio of the two energy densities.

$$factor = \frac{LHV_{NG} * \rho_{NG}}{LHV_{H_2} * \rho_{H_2}} = \frac{38\ \frac{MJ}{kg} * 0.833\ \frac{kg}{m^3}}{120\ \frac{MJ}{kg} * 0.08988\ \frac{kg}{m^3}} = 2.96 \approx 3$$

where $LHV$ is the lower heating value in $MJ/kg$ and $\rho$ is the density in $kg/m^3$ of the gases.

| | |
|---|---|
| Lower Heating Value (LHV) | $120\ \frac{MJ}{kg}$ or $10.78\ \frac{MJ}{m^3}$ |
| Density at STP (101.325 kPa and 15 $^0$C) | $0.08988\ \frac{kg}{m^3}$ |
| Viscosity | 0.87 10-5 $Pa \cdot s$ |

*Table 3-2: Hydrogen gas properties. The properties used for the simulations with Aurora.*

For the natural gas (groningen gas) the value is taken from here [5].

## 3.2 Scenario 1: Local suppliers

In scenario 1, additional suppliers of hydrogen are investigated, as well as their effect on the existing gas network. Considering the areas of Wemeldinge and Kattendjike are more remote areas, located North of Kapelle closer to the coast, it is reasonable to assume that PV or wind parks will be created in the near future. As a result, it is assumed that electrical power from renewable energy sources is used by two electrolyzers, to produce locally hydrogen and inject it into the gas distribution network.

The first electrolyzer is connected to the 4 bar pipelines and the second one to the 100 mbar pipelines. The proposed locations are illustrated below on the figure with black square markers. The electrolyzer added to the North-West branch of the network, is connected on the 4 bar pipeline and it has a hydrogen injection flow of 500 Nm3/h which is approximately the output of a 2 MW electrolyzer. The electrolyzer is supplied by electricity from the wind turbine (green hydrogen) which follows the wind profile. The capacity of the electrolyzer aims to cover the demand of the current branch which has a maximum value between 400-500 Nm$^3$/h. As a result, at the times of the day that demand is lower than maximum, the electrolyzer injects more volume of hydrogen than the demand of the branch. Consequently, the flow through the 4 bar pipeline is reversed. Similarly, an electrolyzer with an output flow of 250 Nm3/h, which is approximately the output of a 1 MW electrolyser, is connected to the small area in the North-East of Kapelle. In this case, the electrolyzer is connected directly to the 100 mbar network. The aim is again to supply with hydrogen to the local area and reduce the dependency to gas supplier 1 and gas supplier 2. In contrast to the first electrolyzer, the capacity of the second electrolyzer is lower, at 250 Nm3/h since it is not possible for a reverse flow to occur through a pressure reducing station.

*Table 3-3 Hydrogen produced for 1 MW and 2 MW electrolyzers*

| Electrolyzer power input (MW$_e$) | Hydrogen produced (Nm$^3$/h) | Efficiency (%) |
|---|---|---|
| 2 | 500 | 75 |
| 1 | 250 | 75 |

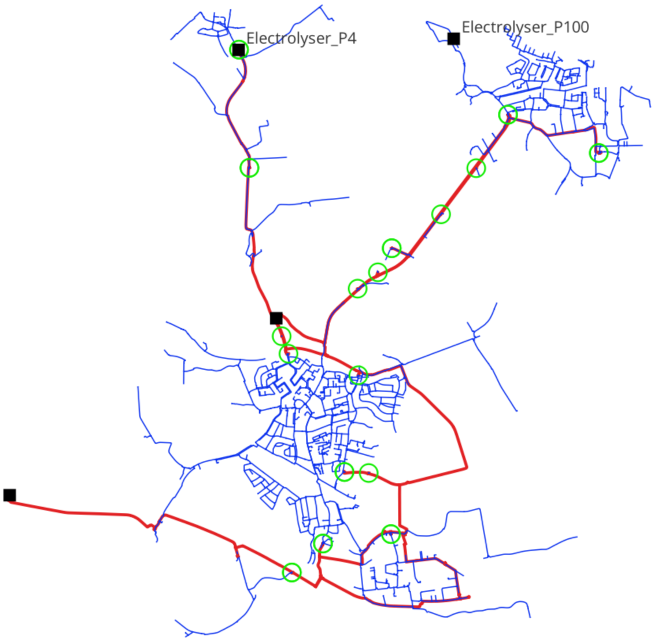


*Figure 3-1 Network for scenario 1. The locations of the added electrolyzers are given with black squares.*

## 3.3 Scenario 2: Pipe break

Scenario 2 focuses on disconnecting the 4 bar pipelines that connect the gas supplier 1 and gas supplier 2 injection points. The deactivation of a pipe simulates an event of maintenance or failure on a 4 bar network that can occur on some rare instances. The pipeline illustrated with black dotted line on the figure below was deactivated for a two main reasons. The first reason is to divide the 4 bar network into two similar parts, one in the South which is connected to gas supplier 2 and another one in the North, which is connected to gas supplier 1. The second reason is to investigate whether the large consumers located in the industrial area, at the South-East of Kapelle, are heavily dependent on the gas supplier 1 injection point. Consequently, the flow direction in the 100 mbar pipelines will change and possibly result in higher flow rates for some instances.

This scenario is in place to show potential bottlenecks in the network, during this kind of unusual events. Some potential observations are, the case where too much demand is asked from one of the two injection points, the case where a big part of the flow finds an alternative route through a smaller pipe, etc. These potential weaknesses of the network may not be immediately visible from scenario 0 where 4 bar network is connecting all areas of Kapelle.

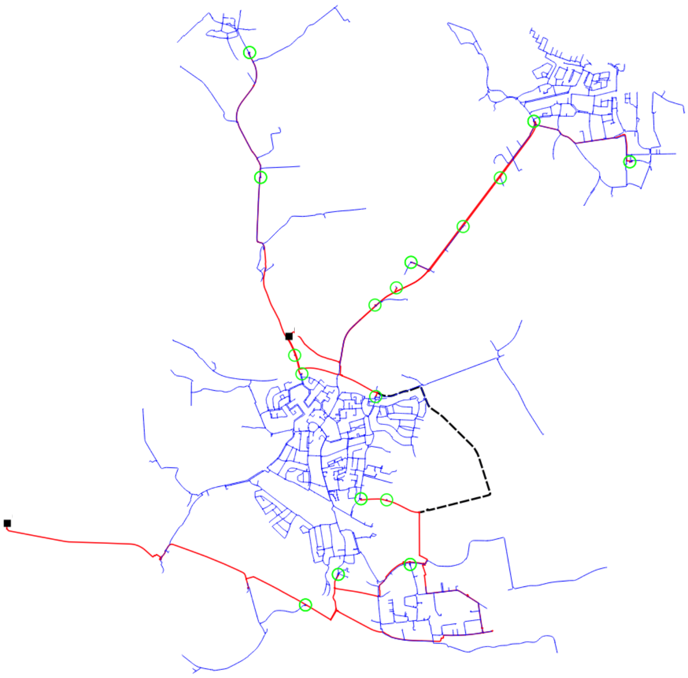

*Figure 3-2 Network for scenario 2. The pipe break is drawn in black dash line*

## 3.4 Scenario 3: Extra industrial demand

In the previous scenarios the demand values for all consumers kept constant while other aspects of the network were modified. The third and final scenario is aiming to provide more insights about the effects of demand on the operation of the gas network. This is achieved by introducing three more hypothetical large consumers to the network, two of them are connected to the 4 bar and one of them on the 100 mbar pipelines. The new consumers are illustrated with orange triangles on the figure with the existing gas network. Therefore, the differences of the network for scenario 3 compared to scenario 0, are the 3 additional large consumers. The rest of the network remains the same.

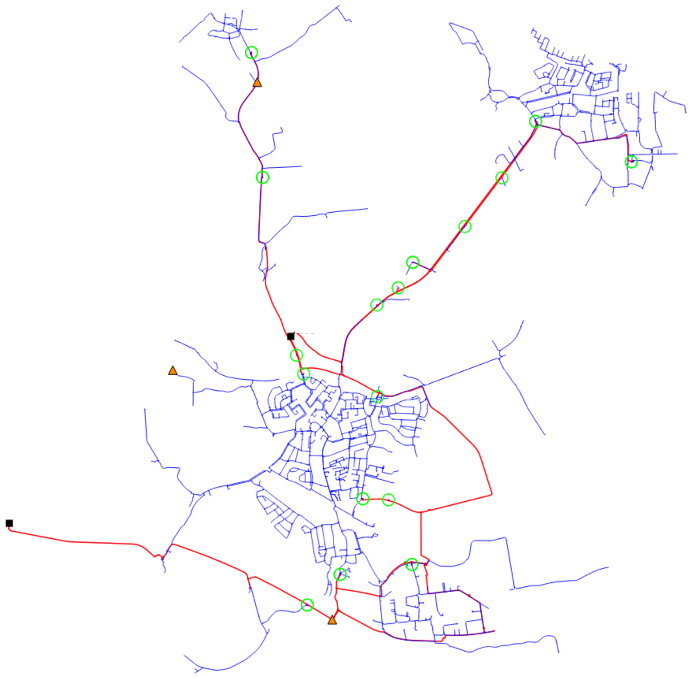

*Figure 3-3 Network for scenario 3. The locations of the new large consumers are given with read triangle.*

The first hypothetical consumer is located on the branch in the North-West of Kapelle and it has a demand flow of 3000 Nm3/h. The demand value is similar to the existing large consumer as the largest one has a peak demand of approximately 5000 Nm3/h in case of hydrogen. By adding a consumer to this branch, the flow rate and pressure drop through this branch will increase drastically. Similarly, the second consumer has a demand of 3000 Nm3/h and is connected to the 4 bar pipeline in the South area of Kapelle, close by the existing industrial area. It simulates an expansion of the industrial area and it aims to investigate if the existing network can operate within the allowable pressure drops and flow rates. The third consumer has a demand of 150 Nm3/h which is lower than the first two, but large compared to other consumers connected to the 100 mbar pipelines. It is connected on a 100 mbar pipe in the middle part of Kapelle area. The purpose is to investigate whether increased flow rates are possible on the low pressure pipelines, for the existing network.

# 4 Results

## 4.1 Gas grid scenario simulation

In this section, we present the consequences for the gas pipeline due to switching from natural gas to hydrogen and several changes on top of that. The results are divided into three category: volumetric flowrate, pressure and flow velocity in the 4 bar and 100 mbar network. The results are presented based on the scenario's defined in Chapter 3. In collaboration with work package 7, we also present the results using Aurora to choose where is the optimal location to place Hydrogen Delivery Station (HDS) from GTS backbone.

Any possible critical points of the network will be evaluated. The increase of volumetric flow rates could result in increasing the pressure drop or increasing the velocity outside of the allowable boundaries (Table 4-1). This is an undesirable effect which is aimed to be prevented by simulating the scenario with great detail with the Aurora simulator. The flow velocity boundary for hydrogen grid is based on study of HyDelta1 WP1E [5] and the pressure boundary is based on Stedin's input. Disclaimer: this value is based on a specific network, in this case Kapelle. Different network will have different criteria. The maximum value of pressure is for the additional hydrogen producer to feed the gas grid. However, the real maximum value of pressure is the design pressure of the pipe. The minimum value is the arrival pressure at station or consumer.

*Table 4-1 Allowable limit for evaluating the network performance*

| Location | Quantity | Minimum Value* | Maximum Value* |
|---|---|---|---|
| **Pipe 4 bar** | Pressure (bar) | 2 | 4 |
| **Pipe 100 mbar** | Pressure (mbar) | 40 | 100 |
| **Pipe** | Velocity (m/s) | - | 60** |

*the value is supplied by Stedin for assessing Kapelle network
** this is based on 3x natural gas limit of 20 m/s from HyDelta1 WP1E

### 4.1.1 Scenario 0: Base scenario

Scenario 0 is expected to show some changes in pressure and volumetric flow rate profiles throughout the network. The values of flow rate are expected to increase by a factor of 3, as the demand of hydrogen is also increased by the same factor. At the same time the distribution of total demand is expected to be the same across the network. For example, the ratio of the flow supplied from gas supplier 1 and gas supplier 2 is expected to be the same. The maximum flowrate in the natural gas network is 4808 Nm³/h and in the hydrogen network is 14425 Nm³/h as shown in Figure 4-1.

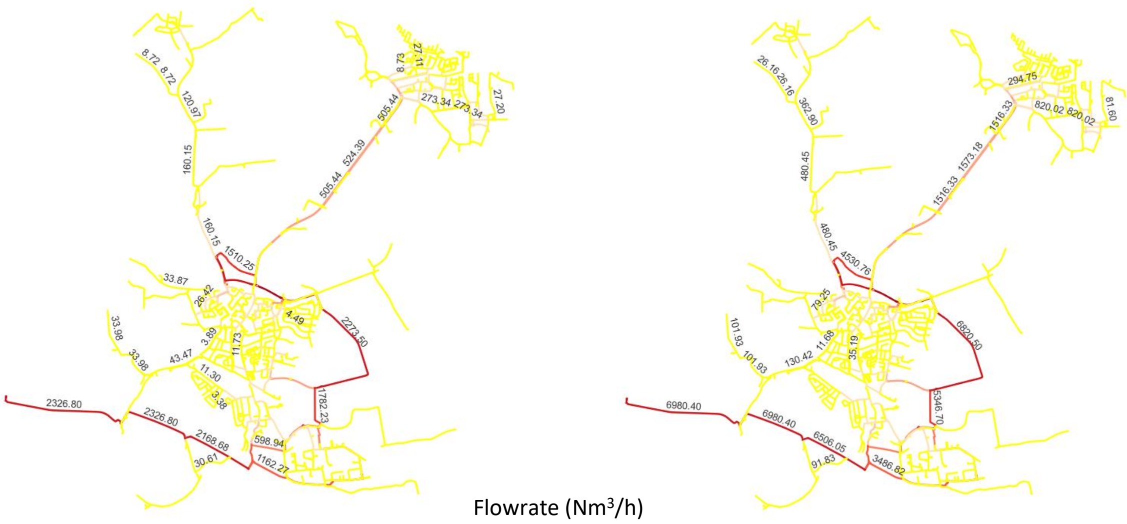

*Figure 4-1 Comparison of flowrate of natural gas (left) and hydrogen (right) in the network*

Next, we evaluate the flow velocity throughout the network. The maximum flow velocity in the natural gas network is 8.9 m/s and the maximum flow velocity in the hydrogen network is 26.5 m/s. The flow velocity of hydrogen pipelines are under their allowable limit 60 m/s.

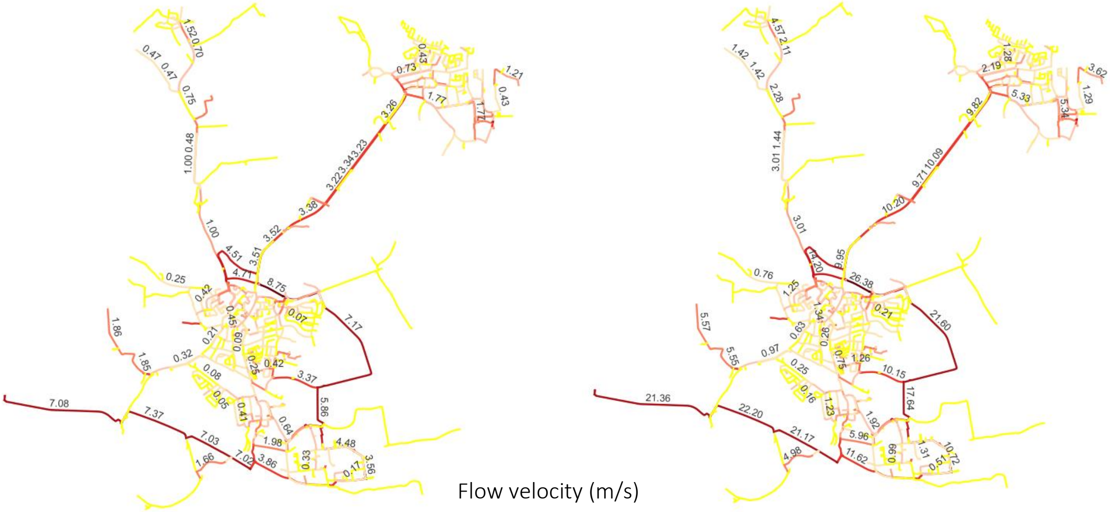


*Figure 4-2 Comparison of flow velocity of natural gas (left) and hydrogen (right) in the network*

The pressure drop between natural gas and hydrogen will be roughly similar due to the pressure drop is direct proportion with density and velocity squared. The density of hydrogen is around 1/9 of the natural gas density, while the velocity of hydrogen in the pipeline is 3 times higher than the natural gas. Figure 4-3 shows the pressure comparison for the 4 bar network between natural gas and hydrogen. The minimum pressure at 4 bar pipelines for natural gas network is 3.06 bar while for hydrogen network is 3.09 bar. Similar behaviour is also found at 100 mbar pipelines. The minimum pressure for natural gas is 74.2 mbar and for hydrogen is 74.9 mbar. (see Figure 4-4)

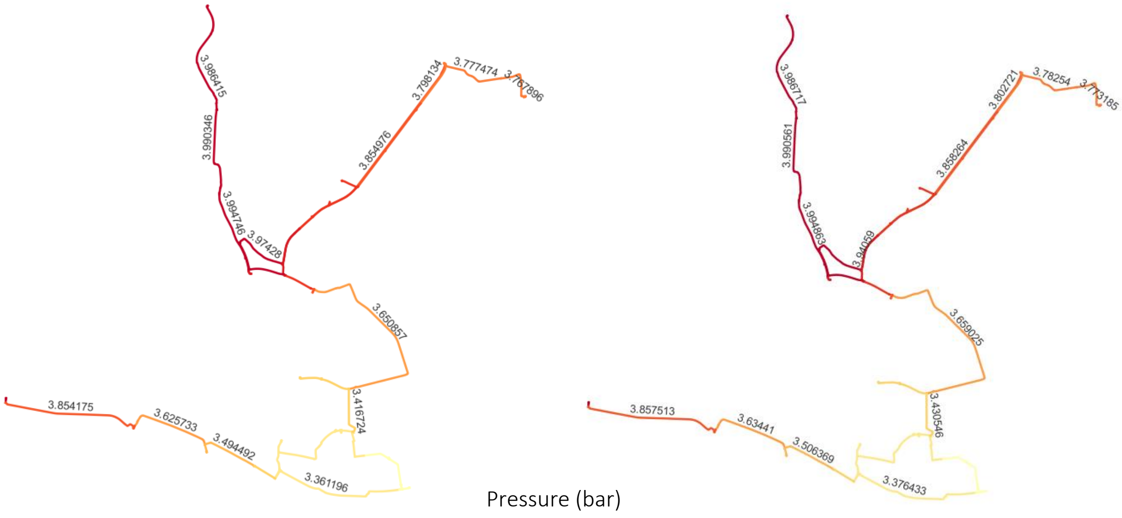


*Figure 4-3 Comparison of pressure at 4 bar pipeline of Natural Gas (left) and Hydrogen (right) in the network*

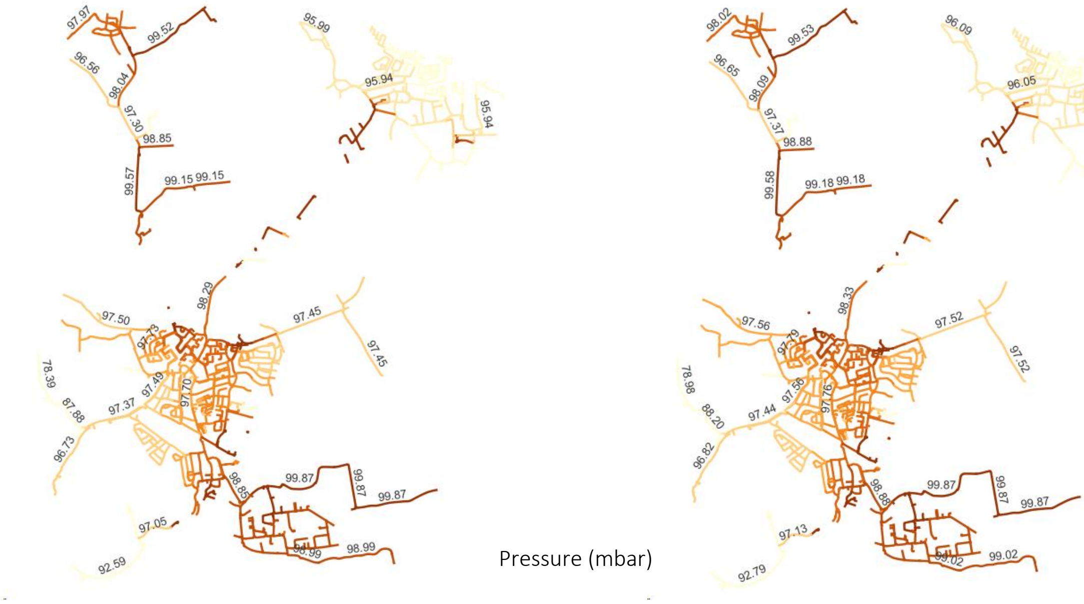


*Figure 4-4 Comparison of pressure at 100 mbar pipeline of natural gas (left) and hydrogen (right) in the network*

Overall observations, even though the flowrate and flow velocity is increased by factor of 3 in the hydrogen grid, the pressure in the hydrogen grid will be similar like the natural gas network.

### 4.1.2 Scenario 1: Local suppliers

Scenario 1 is focusing on a future scenario where there will be several decentralized electrolyzers connected to renewable electricity producer (e.g. wind turbines or solar park) to feed the hydrogen grid. In this scenario, both electrolyzers are connected to 2 MW and 1 MW wind turbines directly, without external grid power (Figure 4-5). The power generated by the wind turbine is following the wind speed using cut-in at 4 m/s and rated speed at 12 m/s (Figure 4-6). The power curve then is scaled to wind turbine capacity in terms of MW (Figure 4-7).

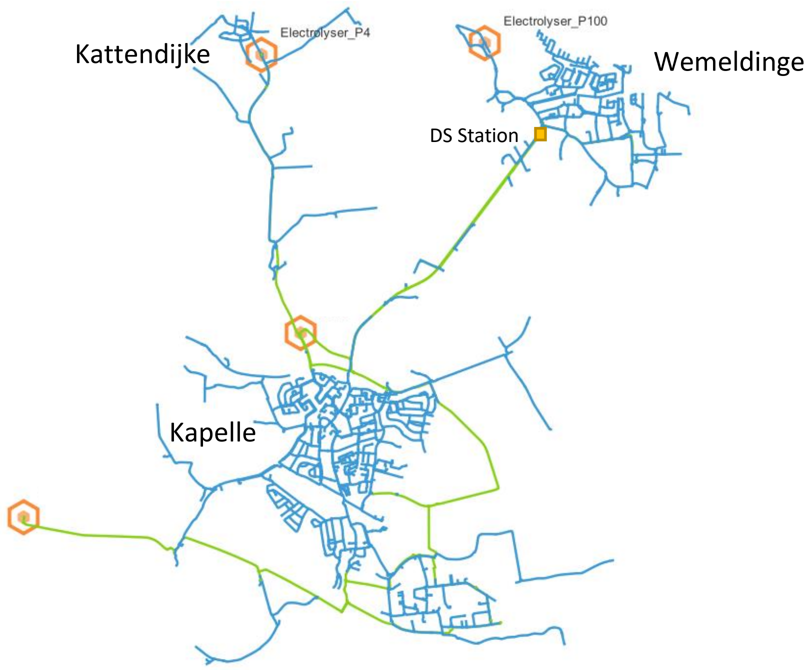


*Figure 4-5 Local eletrolyzers location in the Kapelle network at 4 bar and 100 mbar network*

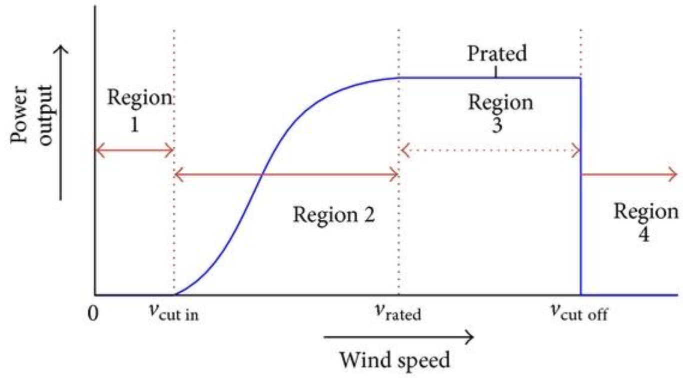


*Figure 4-6 Typical power curve generated by the wind turbine based on wind speed*

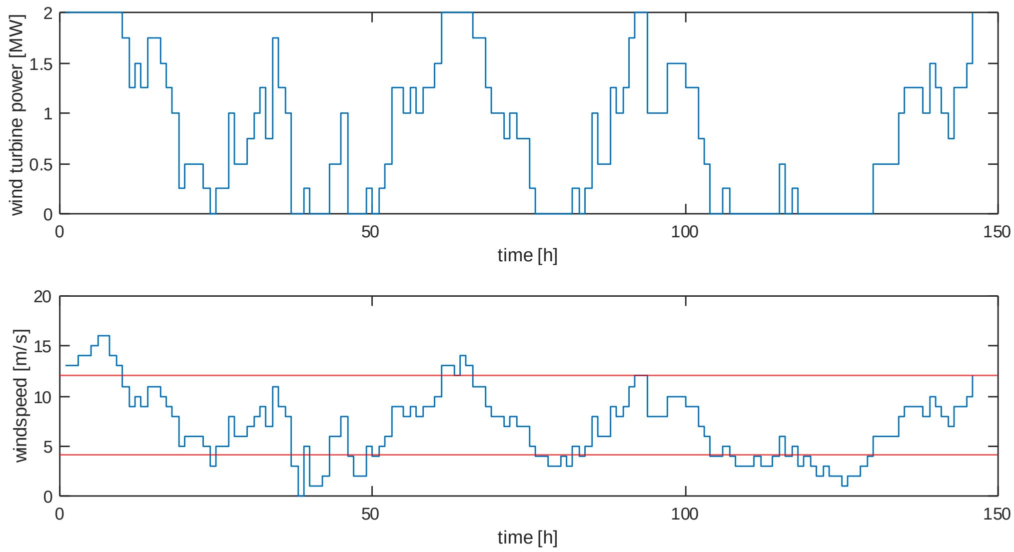


*Figure 4-7 Intermittent electricity production of 2 MW wind turbine with respect to wind speed profile.*

Then, we run simulation for two days in order to see the dynamic results of electrolyzer supply in the 4 bar and 100 mbar network respectively. Figure 4-8 shows the pressure and flow for a 2 MW eletrolyzer. The maximum pressure is still below the allowable limit (see Table 4-1) during maximum production during the night. The hydrogen flow produced from the electrolyzer is based on availability of the renewable electricity from wind. During the first night, the electrolyzer is able to supply whole the Kattendijke demand and the surplus is supplied back to the South as you can see negative flow in the 4 bar pipe supplying Kattendijke. When there is no wind situation (at hour 40), the flow from South is supplying the Kattendijke area.

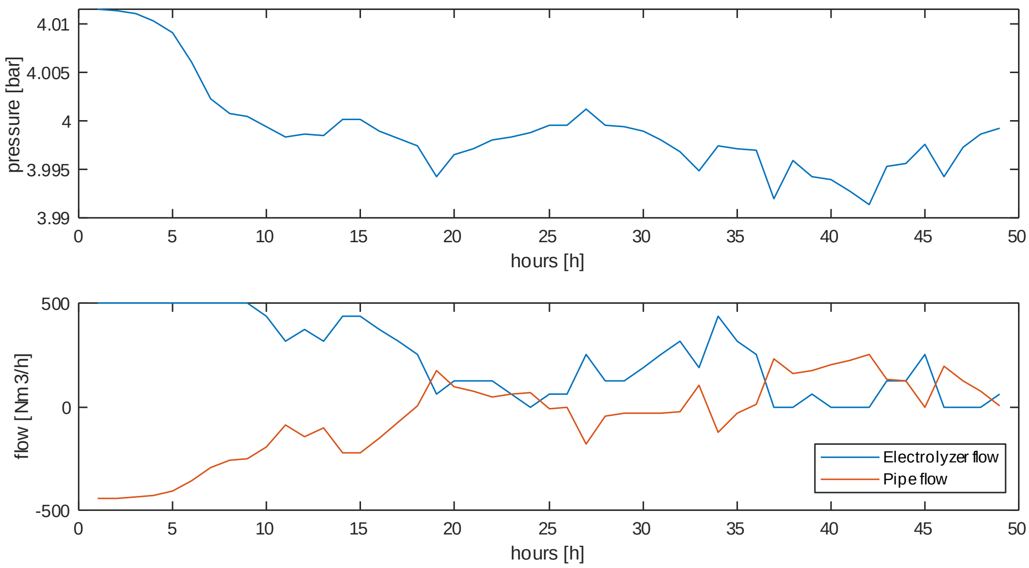


*Figure 4-8 The 2 MW electrolyzer pressure and flow at 4 bar network*

Similar with the Wemeldinge area, the maximum pressure of electrolyzer is still below allowable limit (Figure 4-9). The bottom graph shows the hydrogen flow at the electrolyzer, nearby pipe and also the district station at Wemeldinge. At the nearby pipe (red line), the flow is reversed when there is high flow from electrolyzer (blue line). Since district station has no compressor, it is not allowed to have reverse flow at the station. For the 1 MW electrolyzer, the total demand at Wemeldinge area during the night and day is always higher than the electrolyzer flow.

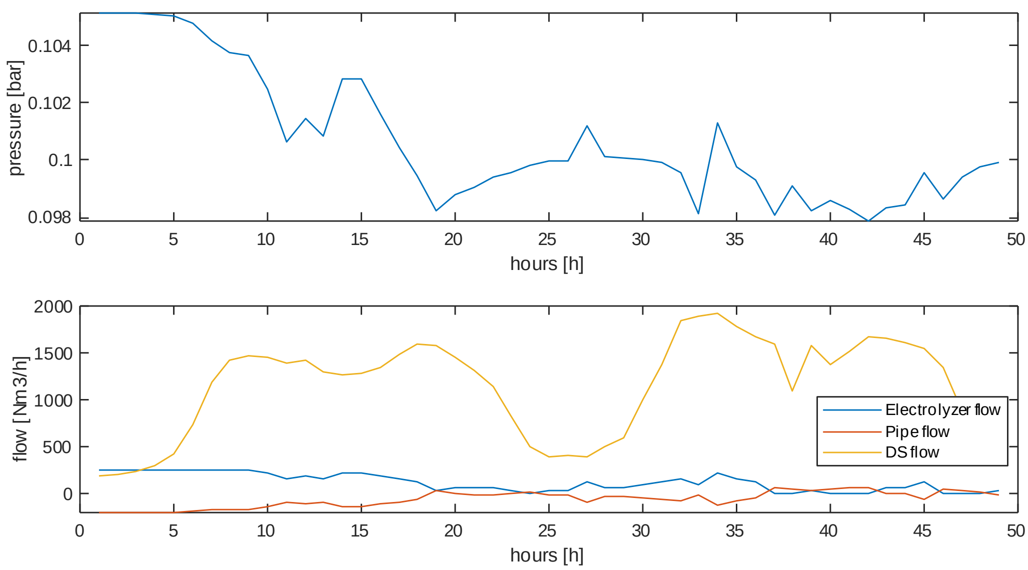


*Figure 4-9 The 1 MW electrolyzer pressure and flow at 100 mbar network*

The same approach can also be used to evaluate where to put the electrolyzer and to determine the size of the electrolyzer before reaching the allowable pressure limit in the system. It also can be used to quantity how often there is a reverse flow in a certain area or station.

We also can add flexibility for electricity supply for an electrolyzer using an external grid. For example, if the electricity from the renewable source is below the base load, then it uses the electricity from the external grid to keep the electrolyzer still delivering the hydrogen.

### 4.1.3 Scenario 2: Pipe break

The simulation model of the network also can be used to evaluate the performance of the network in the case of maintenance or an unexpected event. N-1 contingency analysis is performed by removing a pipe or station from the network to evaluate the impact. Using this approach, the operator will gain knowledge upfront regarding the consequence of the event to guarantee security of supply.

The base scenario result shows that the industrial cluster area in the south east is supplied both from gas supplier 1 and gas supplier 2 (see Figure 4-10). The gas supplier 1 contribute 67% of the total demand and the gas supplier 2 is 33%. Due to a pipe break, the industrial area is mainly supplied by the gas supplier 2. The flow contribution of gas supplier 2 is now 59% compared to the gas supplier 1 is 41% (see Figure 4-11).

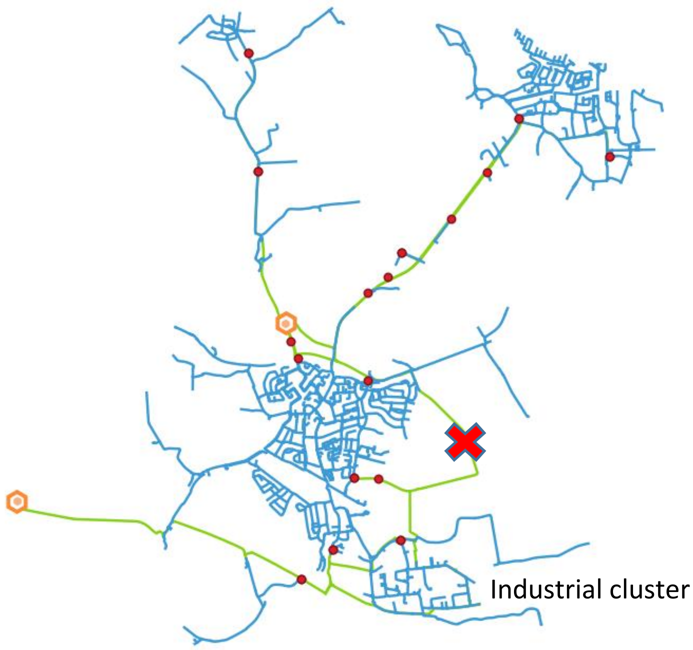


*Figure 4-10 Location of pipe break at 4 bar network (red cross)*

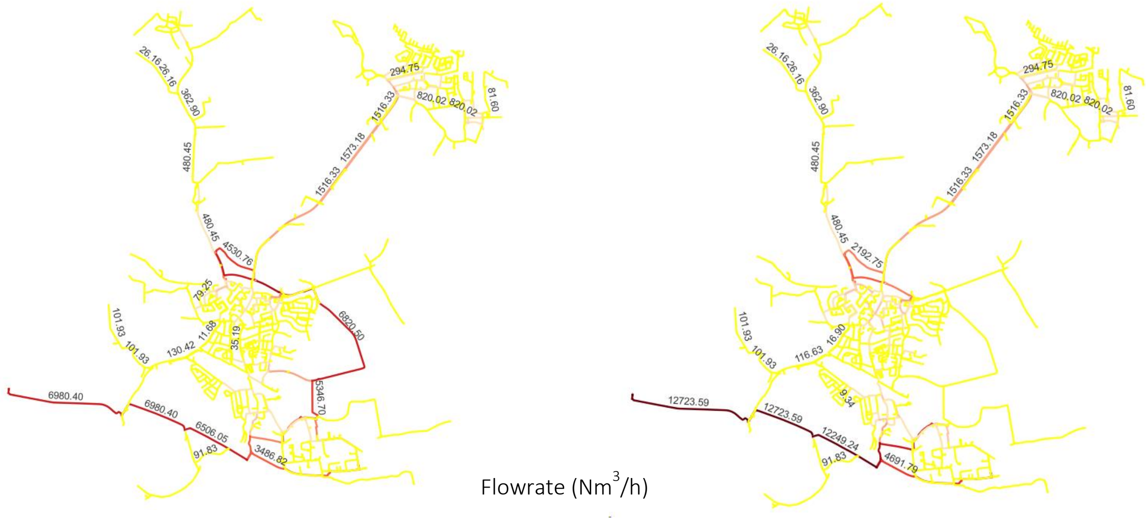


*Figure 4-11 Hydrogen flow comparison base scenario (left) and pipe break scenario (right). The flow coming from gas supplier 2 is doubled*

Due to high flowrates from the gas supplier 2 station, the lowest pressure near the large consumer at the industrial area is 1.1 bar (Figure 4-12 green circle). This is not an acceptable pressure value for a 4 bar grid. Thus this pipe is really critical to be monitored.

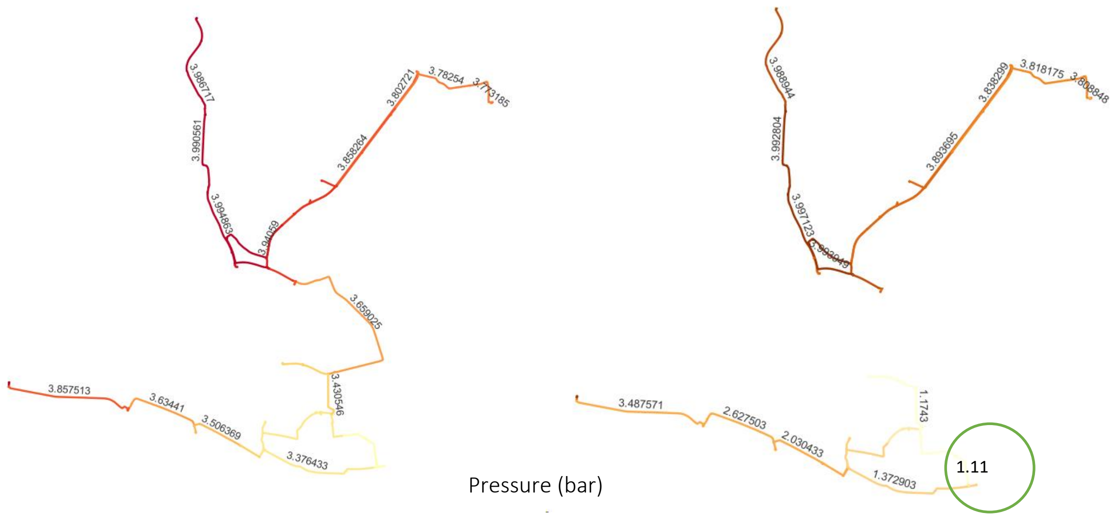


*Figure 4-12 Comparison of pressure at 4 bar pipeline base scenario (left) and pipe break scenario (right)*

### 4.1.4 Scenario 3: Extra industrial demand

Adding additional extra industrial demand will give a different pressure distribution in the grid. The simulator can be used to check if it is possible to add additional connections to the grid for large consumer.

We add three large consumers: two consumers are at the 4 bar pipeline and one consumer is at the 100 mbar pipeline (see Figure 4-13). Additional total ~8000 Nm$^3$h of hydrogen is added to the peak demand compared to Scenario 0. The result is shown in Figure 4-14 and Figure 4-15 for pressure at the 4 bar pipeline and the 100 mbar pipeline respectively.

*Figure 4-13 Location of additional large consumers in the 4 bar network (red triangle) and 100 mbar network (red cross)*

In the 4 bar network, the minimum pressure in the system drops from 3.09 bar to 2.27 due to additional large consumers in the South part of the network. This might be slightly lower than the limit at 4 bar pipeline (see Table 4-1). We also see that the pressure in the Kattendijke DS station drops from 3.95 to 3.25 bar (Figure 4-14 green circle). Then, it is still possible to have a large consumer in the 4 bar pipeline near this area.

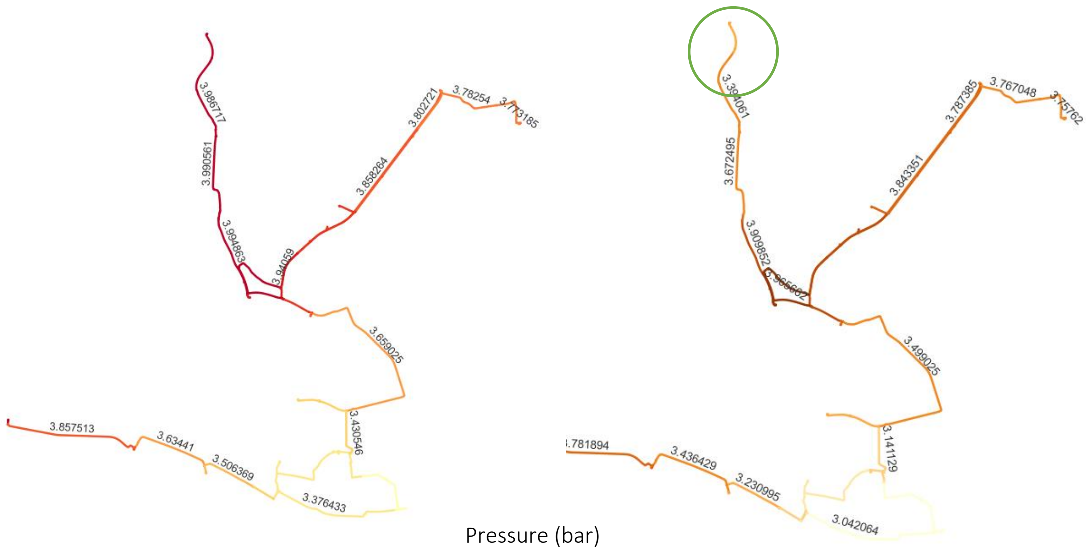


*Figure 4-14 Comparison of pressure at 4 bar pipeline of Scenario 0 (left) and Scenario 3 (right) in the network*

In the 100 mbar network, the lowest pressure is 66.7 mbar at the large consumer (Figure 4-15 green circle). Adding a large consumer with 150 $Nm^3/h$ is still acceptable in the grid.

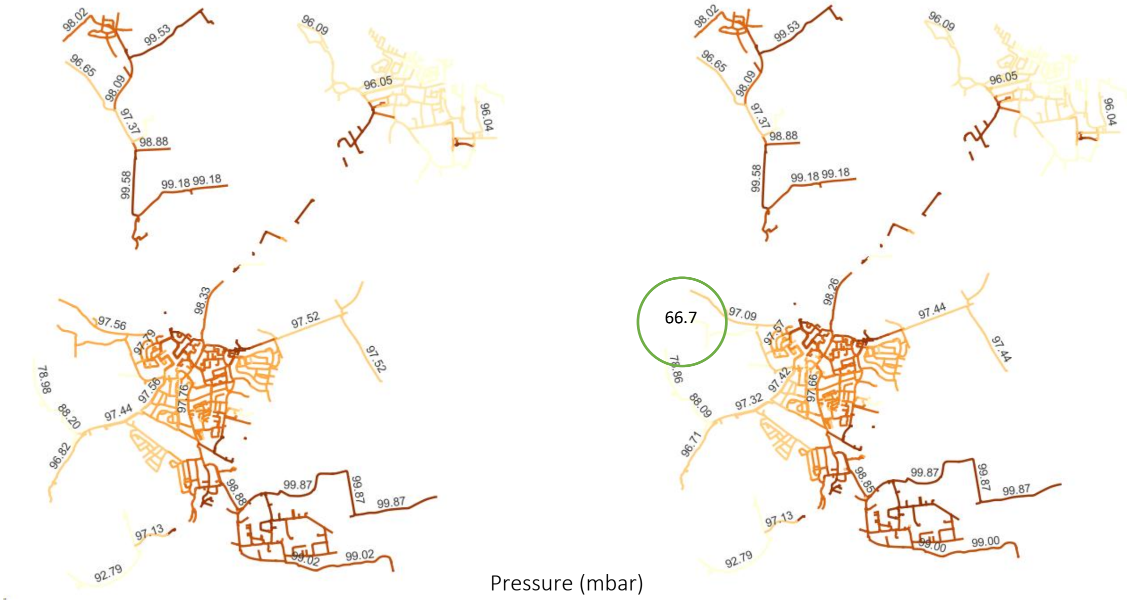


*Figure 4-15 Comparison of pressure at 100 mbar pipeline of Scenario 0 (left) and Scenario 3 (right) in the network*

### 4.1.5 Scenario WP7: Hydrogen Delivery Station

The scenario is to have the Hydrogen Delivery Station at the south east near the industrial area to supply hydrogen throughout the network (Figure 4-16). The gas supplier 1 and the gas supplier 2 will be shut off. So, there is only one location supplying the network.

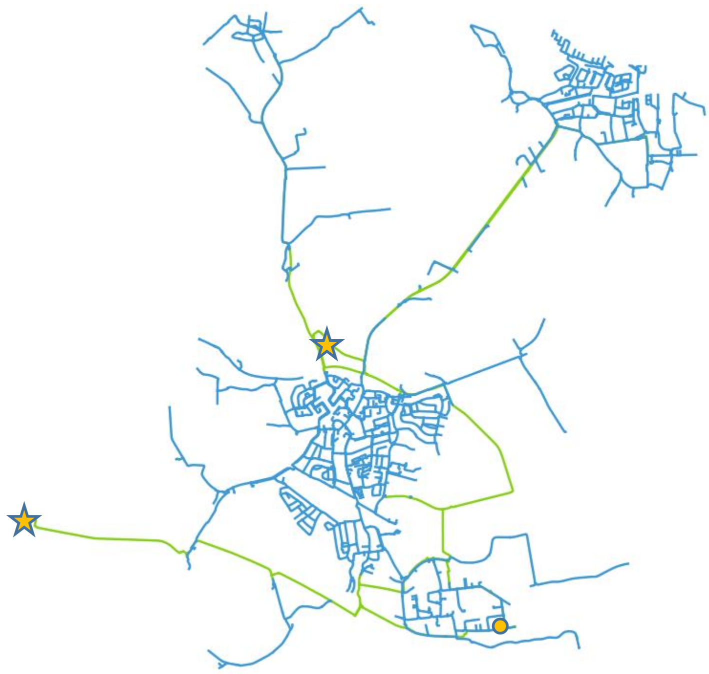

*Figure 4-16 Location of the hydrogen delivery station (yellow circle) and the gas supplier 1 and gas supplier 2 is shut off (yellow star)*

Looking at the pressure in the 4 bar network, the minimum inlet pressure at DS station in the north east is 1.74 bar (see green circle in Figure 4-17). This is below the standard guideline of allowable limit for 4 bar network which is 2.5 bar. The minimum pressure in the 100 mbar network is 73.71 mbar. This is an acceptable value.

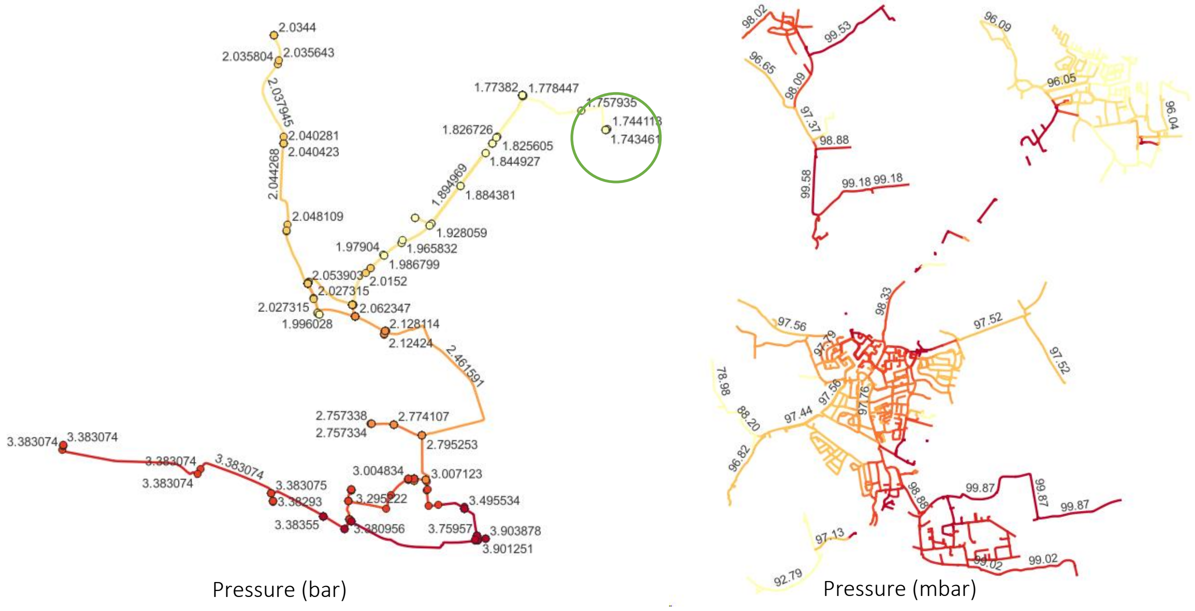


*Figure 4-17 Pressure distribution at 4 bar (left) and 100 mbar (right) pipelines in the network for the hydrogen delivery station in the south east.*

If we look into the flow velocity in the network, most values are below 60 m/s. However there is a pipe segments with DN100 with a flow velocity of around 72 m/s (see Figure 4-18 green circle). Both locations are near to the hydrogen delivery station. Replacement of the pipe into a bigger diameter is needed in order to reduce the flow velocity.


*Figure 4-18 Flow velocity in the network for the hydrogen delivery station in the south east.*

Beside implementing a bigger pipe diameter to reduce pressure drop and flow velocity, another mitigation approach is by finding another optimal location for the hydrogen delivery station. Thus, we are moving the location slightly to the north as seen in Figure 4-19.

*Figure 4-19 Location of the new hydrogen delivery station (yellow circle) in the north of industrial area at 4 bar pipeline.*

By moving the location of hydrogen delivery station a bit to the north in the 4 bar pipeline, it solves all the problems except the flow velocity at the south east large consumer. Now, the minimum inlet pressure at DS station in the 4 bar pipeline is 3.13 bar and in the 100 mbar pipeline is 73.7 mbar (Figure 4-20). The maximum flow velocity in the network is 37.8 m/s (Figure 4-21).

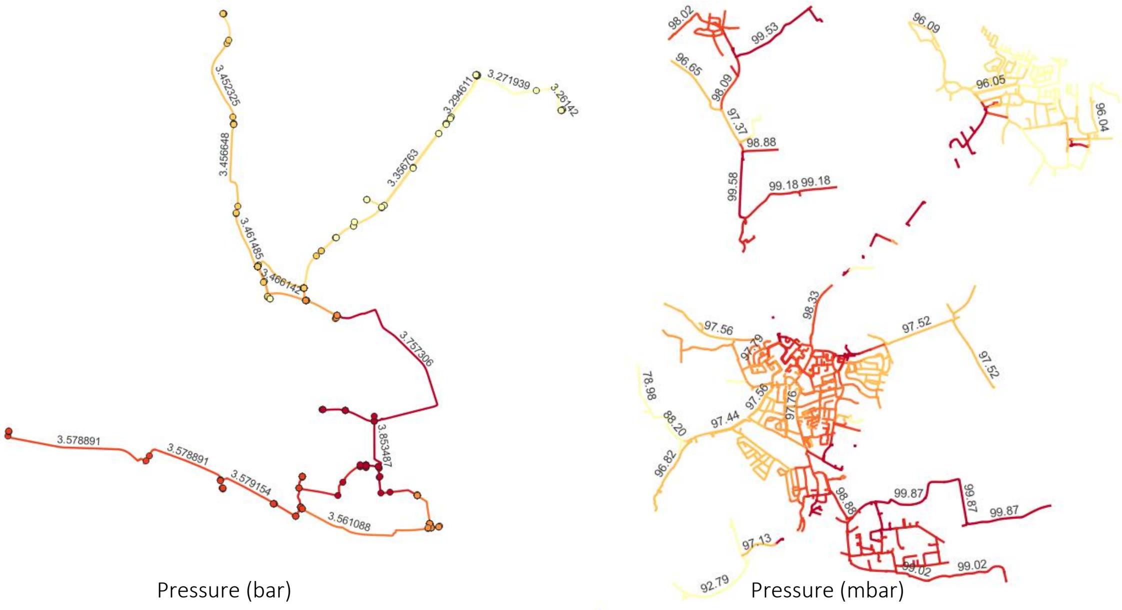


*Figure 4-20 Pressure distribution at 4 bar (left) and 100 mbar (right) pipelines in the network for the new location of hydrogen delivery station*


Flow velocity (m/s)

*Figure 4-21 Flow velocity in the network for the new location of hydrogen delivery station.*

## 4.2 Optimal pressure sensor placement

In this chapter, the results for the optimal pressure sensor placement are presented and explained. The location of pressure sensors is estimated from the optimization algorithm, where the possible sensor locations are defined. The allowable sensor locations are the pressure reducing station locations, for two reasons. The main reason is that the outlet pressure of the stations is fixed to 100 mbar, therefore, any pressure variations that cause uncertainty is canceled out. Consequently, the aim is to reduce the uncertainty for the pressure values for the 4 bar network. The second reason is a practical reason. Stations are the only instances in the network where hydrogen pipes are above the ground and easy to access. This makes the installation of sensors simpler.

The second part of the results is the reduction of uncertainty. For each scenario, a curve that illustrates this reduction is given. It shows the value of total pressure uncertainty or standard deviation in the network, including the 4 bar and 100 mbar pipes. As it was mentioned in previous chapters, the total uncertainty (the same as total standard deviation) is calculated with the sum of the standard deviations of all nodes. For the introduction of the results in the chapters below, the term total uncertainty is used.

### 4.2.1 Scenario 0: Base scenario result

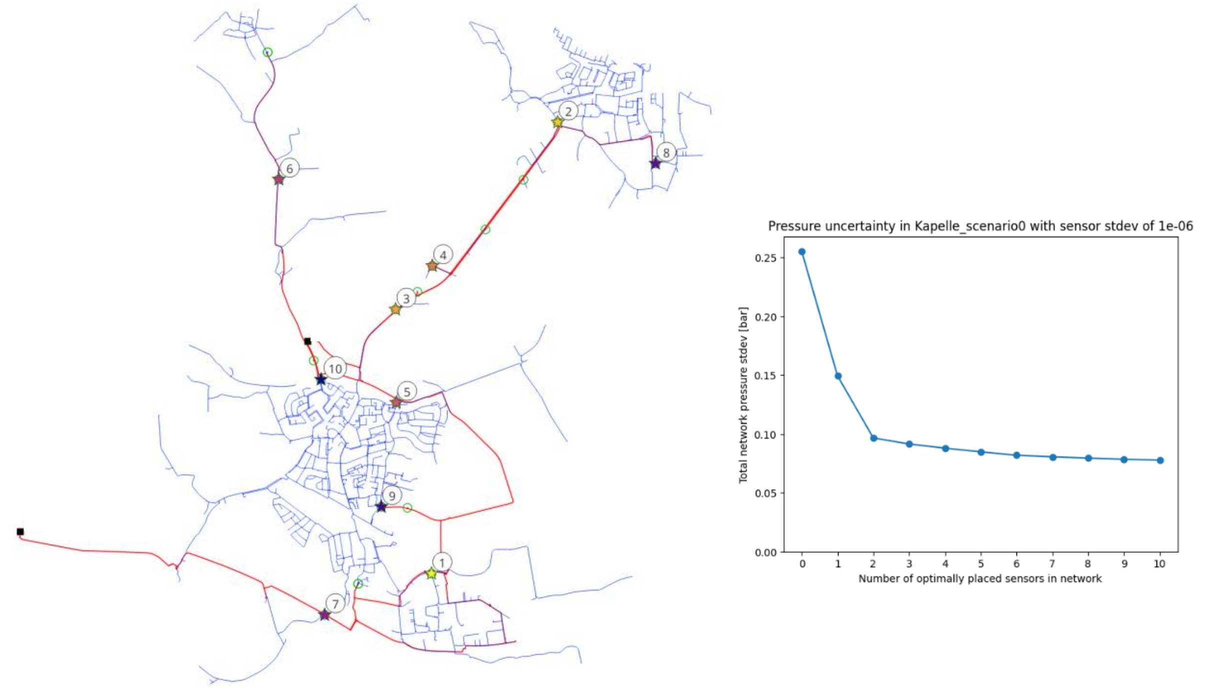


*Figure 4-22: Optimal pressure sensor placement of 10 sensors for scenario 0, in the network of Kapelle (left). The coloured stars show the locations of the sensors and the green circles indicate the possible sensor locations, which are the locations of the stations. Reduction of total pressure uncertainty as a function of the number of optimally placed sensors (right).*

In Figure 4-22, the stars show the locations of the pressure sensors. The numbers next to the stars give the order for the optimal sensor placement. For example, if the operator of the network wants to place 4 sensors in this area, sensor locations 1, 2, 3 and 4 are the preferred locations, suggested by the optimization algorithm.

The first sensor is placed on the South-East part of the network, near the industrial area with big consumers and it is illustrated with light yellow star. The second and third sensors are placed on the branch connecting the North-East area. From the curve of total pressure uncertainty in the network, we observe a steep increase for sensors 1 and 2. For sensors 3 to 10, the decrease is becoming smaller and smaller.

Comparing the values of uncertainty, in is worth to mention that the pressure uncertainty decrease drastically by placing the 1st and 2nd sensors. The decrease of pressure uncertainty is observed in the nearby area and in the path from the hydrogen supply, gas supplier 1 and gas supplier 2, to the sensor. Similarly, the uncertainty decreases in the area closer to gas supplier 1 when the 3rd sensor is added, but it is not as obvious because the pipelines from the gas supplier 1 to the stations are shorter. The illustration of the pressure uncertainty reduction can be found in the appendix 8.1.

### 4.2.2 Scenario 1: Local suppliers result

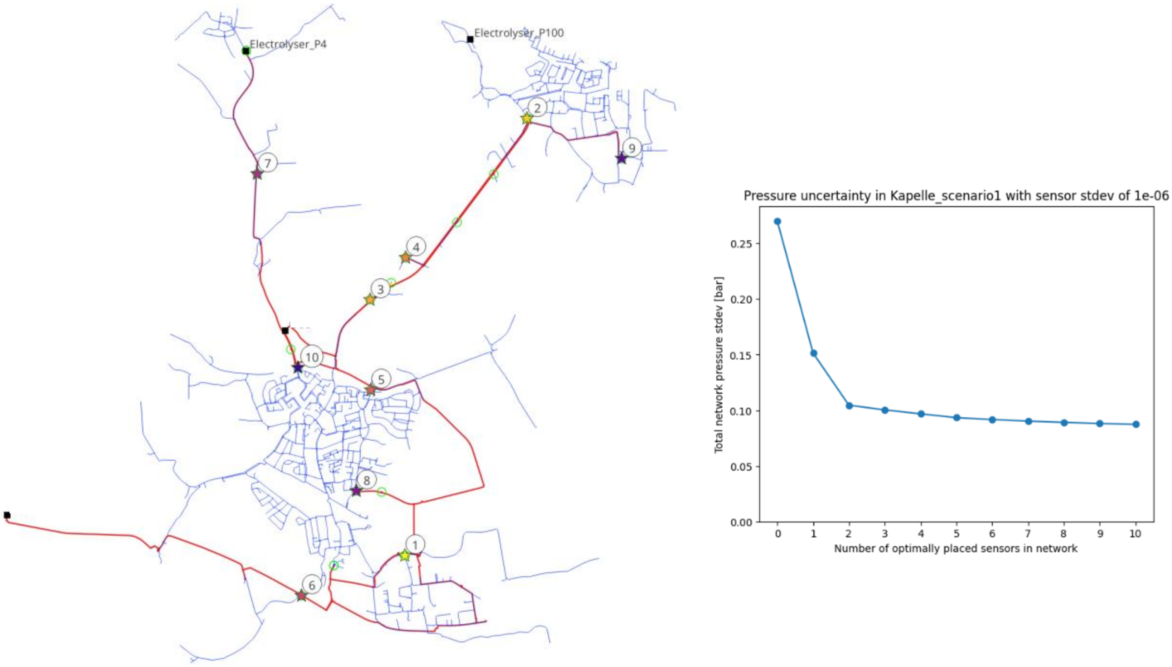


*Figure 4-23: Optimal pressure sensor placement of 10 sensors for scenario 1, in the network of Kapelle (left). The coloured stars show the locations of the sensors and the green circles indicate the possible sensor locations, which are the locations of the stations. Reduction of total pressure uncertainty as a function of the number of optimally placed sensors (right).*

For scenario 1, where two electrolysers were added to the network, the effect of the placement of the first three pressure sensors is the same as in scenario 0. Furthermore, by comparing the pressure uncertainty curve for scenarios 0 and 1, a similar behaviour is observed. More specifically, on Figure 4-23, the first sensor decreases the total pressure uncertainty the most, from a value of about 0.27 bar to 0.15. Then, for every additional sensor, the decrease is smaller.

Each sensor aims to decrease the uncertainty of a different area. For example, pressure sensor 1 targets the industrial area in the South-East part of Kapelle where the large hydrogen consumers are located. Moreover, each sensor improves the uncertainty values in the area nearby but also the uncertainty in the paths from gas supplier 1 and gas supplier 2 towards the sensor location.

### 4.2.3 Scenario 2: Pipe break result

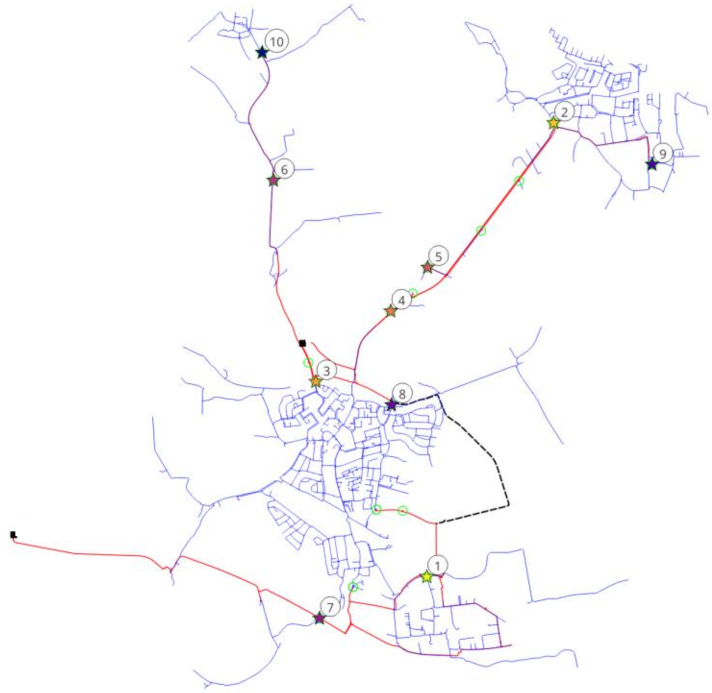


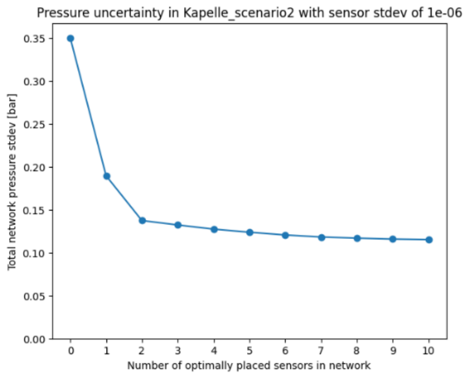


*Figure 4-24: Optimal pressure sensor placement of 10 sensors for scenario 2, in the network of Kapelle (left). The coloured stars show the locations of the sensors and the green circles indicate the possible sensor locations, which are the locations of the stations. Reduction of total pressure uncertainty as a function of the number of optimally placed sensors (right).*

For scenario 2, a 4 bar pipeline is shut-off to divide the 4 bar network into two parts. From Figure 4-24, the first two sensors are in the same locations as scenario 0. In contrast, sensor number 3 is placed in a different location. Specifically, sensor 3 is located in a station near the gas supplier 1 that supplies the central part of Kapelle.

The 1st and 2nd sensors show a decrease of pressure uncertainty in the South-East and North-East parts of the network, respectively. The 3rd sensor has a visible impact only on a short pipe of the 4 bar network. In addition, the curve of total pressure uncertainty shows a higher initial value, compared to scenario 0. In addition, the first 2 sensors have the most impact on the total uncertainty. Sensors 3 to 10 have only a marginal impact.

#### 4.2.4 Scenario 3 Extra industrial demand result

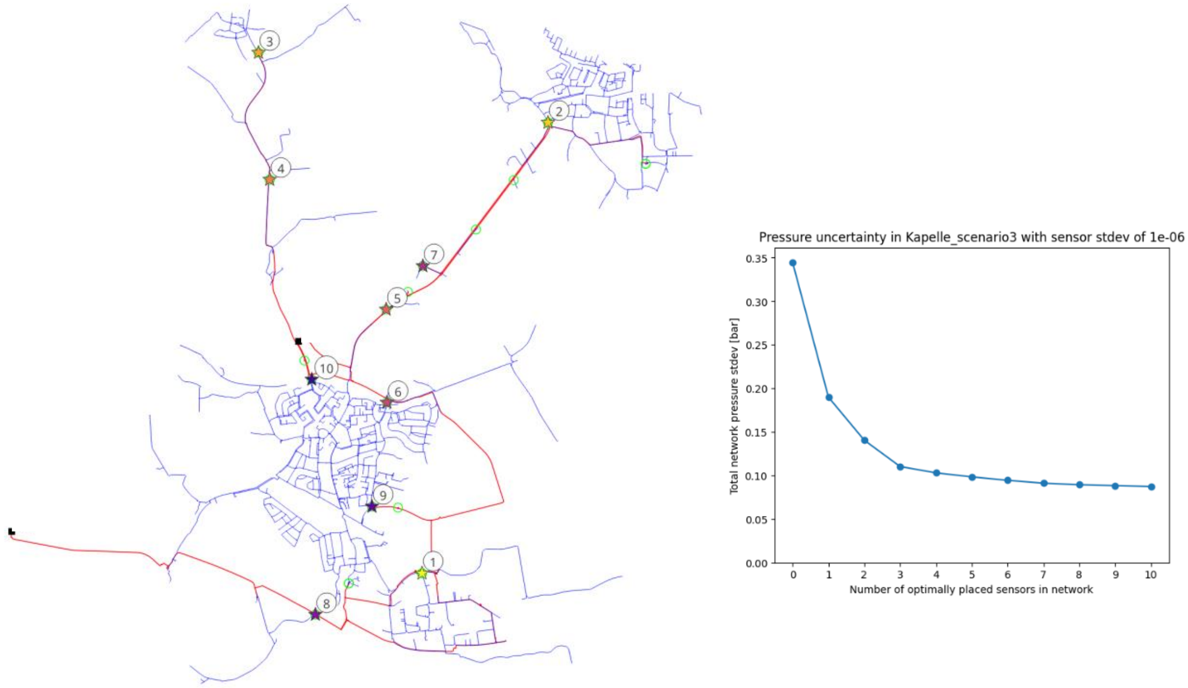


*Figure 4-25: Optimal pressure sensor placement of 10 sensors for scenario 3, in the network of Kapelle (left). The coloured stars show the locations of the sensors and the green circles indicate the possible sensor locations, which are the locations of the stations. Reduction of total pressure uncertainty as a function of the number of optimally placed sensors (right).*

Scenario 3 is about adding three new large consumers in the network. As it is illustrated on Figure 4-25, the result of the pressure sensor placement for sensors 1 and 2 is the same to scenario 0. In this case the initial value of the total pressure uncertainty is higher, at approximately 0.35 bar. At the same time, a similar rate of decrease in pressure uncertainty is observed, with a difference in the impact of the 3rd sensor. For scenario 0, the addition of a 3rd sensor resulted in a smaller decrease of uncertainty whereas for scenario 3, the decrease is higher.

For scenario 3 the distribution of uncertainty is different throughout the network of Kapelle. The two branches in the North part of the network, show higher initial pressure uncertainty relative to scenario 0. This higher uncertainty decreased drastically by placing sensors 2 and 3.

### 4.3 Optimal flow sensor placement

In the current chapter, the results for the optimal flow sensor placement are presented. The possible sensor locations are the pressure reducing stations, same as in the previous chapter. The reason is that is practical to place the sensors in the stations, as there is easy access. Furthermore, the possible sensor locations are the same with the pressure sensor placement, so a comparison of the optimal sensor locations is possible between the two studies.

Initially, the flow sensor placement of the first 10 sensors is presented for each scenario. Additionally, a curve is included in the results, illustrating the total flow uncertainty (total flow standard deviation) as a function of the number of optimally places flow sensor. The total flow uncertainty or total flow standard deviation is calculated with the sum of the flow standard deviations of all pipes in the network, including the 4 bar and the 100 mbar pipes.

### 4.3.1 Scenario 0: Base scenario result

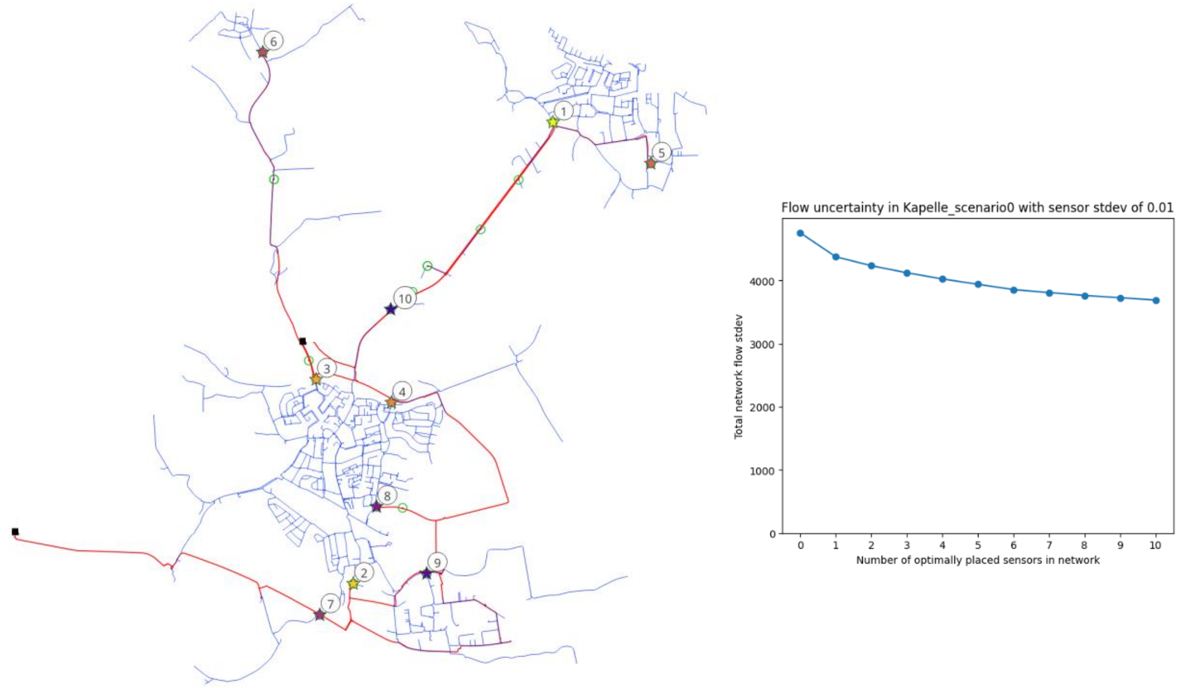


*Figure 4-26: Optimal flow sensor placement of 10 sensors for scenario 0, in the network of Kapelle (left). The coloured stars show the locations of the sensors and the green circles indicate the possible sensor locations, which are the locations of the stations. Reduction of total flow uncertainty as a function of the number of optimally placed sensors (right).*

Results for flow sensor placement, for scenario 0 are illustrated with Figure 4-26. The total uncertainty of ~5000 Nm3/h is the sum of uncertainty in all pipes (while for a single pipe, the maximum uncertainty is 10 $Nm^3/h$). In the left subfigure, the optimal location placement is presented. The 1st sensor is placed by the optimization algorithm in the North-East area, where mostly small consumers are located. The 2nd sensor is placed in the South part of the network, close to the industrial area. The 3rd sensor is placed in a short distance from gas supplier 1 injection point, to the South.

Regarding the curve of total flow uncertainty, the decrease of the value is relatively not steep. The 1st sensor has the biggest impact on the total uncertainty and the last sensor the smallest. The placement of the 1st sensor in the North-East area has an impact on flow uncertainty on the area nearby and on the path towards the gas supplier 1. The 2nd sensor has a similar reduction of uncertainty in the South part of Kapelle. The illustration of the flow uncertainty reduction can be found in the appendix 8.2

### 4.3.2 Scenario 1: Local suppliers result

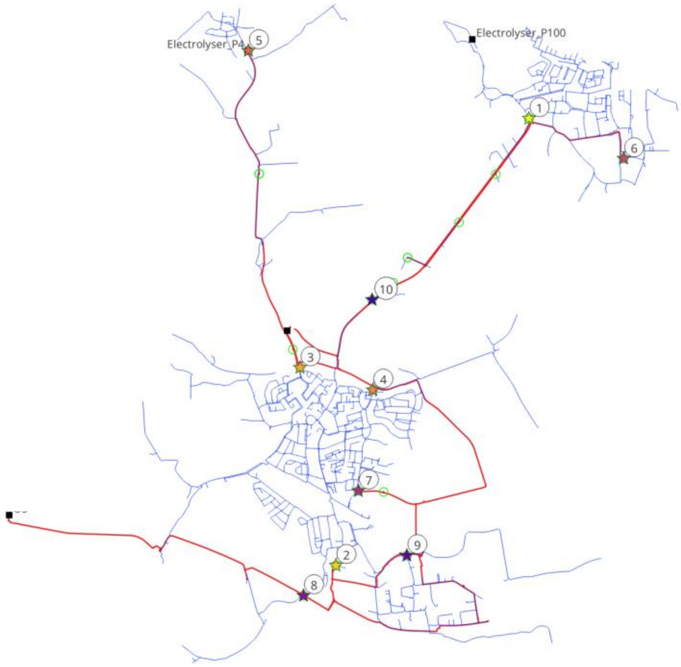


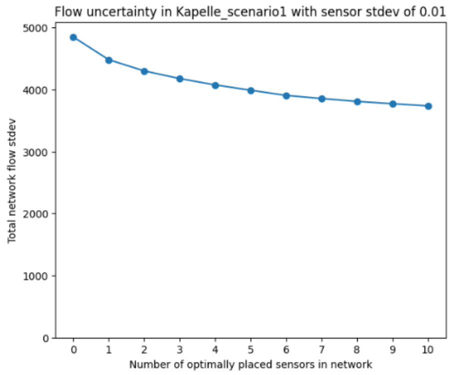


*Figure 4-27: Optimal flow sensor placement of 10 sensors for scenario 1, in the network of Kapelle (left). The coloured stars show the locations of the sensors and the green circles indicate the possible sensor locations, which are the locations of the stations. Reduction of total flow uncertainty as a function of the number of optimally placed sensors (right).*

The flow sensor placement results for scenario 1 are illustrated in Figure 4-27. The sensor locations are shown in the left subfigure, where the location of the electrolysers are also given. For sensors 1, 2, 3 and 4 the locations are the same as in the scenario 0. A different curve is observed compared to scenario 0 in the right subfigure. The behaviour of total flow uncertainty is similar as the decrease of the value is gradual whereas the total flow uncertainty values area higher of all number of sensors. For example, the total flow uncertainty for 0 optimally placed flow sensors is approximately 4900 $Nm^3/h$ whereas for scenario 0 it is approximately 4700 $Nm^3/h$.

### 4.3.3 Scenario 2: Pipe break result

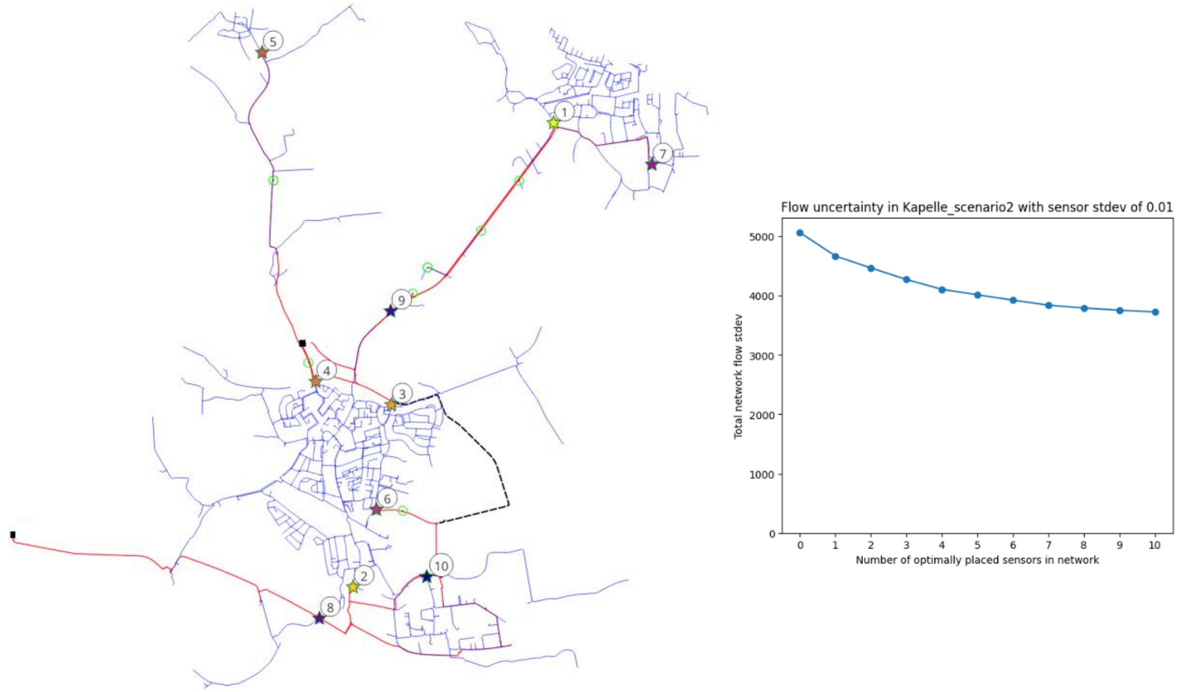


*Figure 4-28: Optimal flow sensor placement of 10 sensors for scenario 2, in the network of Kapelle (left). The coloured stars show the locations of the sensors and the green circles indicate the possible sensor locations, which are the locations of the stations. Reduction of total flow uncertainty as a function of the number of optimally placed sensors (right).*

The results of flow sensor placement for scenario 2, are illustrated in Figure 4-28. For the current scenario sensors 1 and 2 are placed in the same locations as in scenario 0, whereas, sensor 3 is placed in a station close from gas supplier 1, which supplies with hydrogen the middle part of Kapelle. The sensor 3 is also located where the disconnected 4 bar pipe is normally connected to the 4 bar network. Furthermore, as the right subfigure suggests, the values of total flow uncertainty are higher overall and the decrease of uncertainty for every additional sensor is steeper compared to scenario 0.

### 4.3.4 Scenario 3: Extra industrial demand result

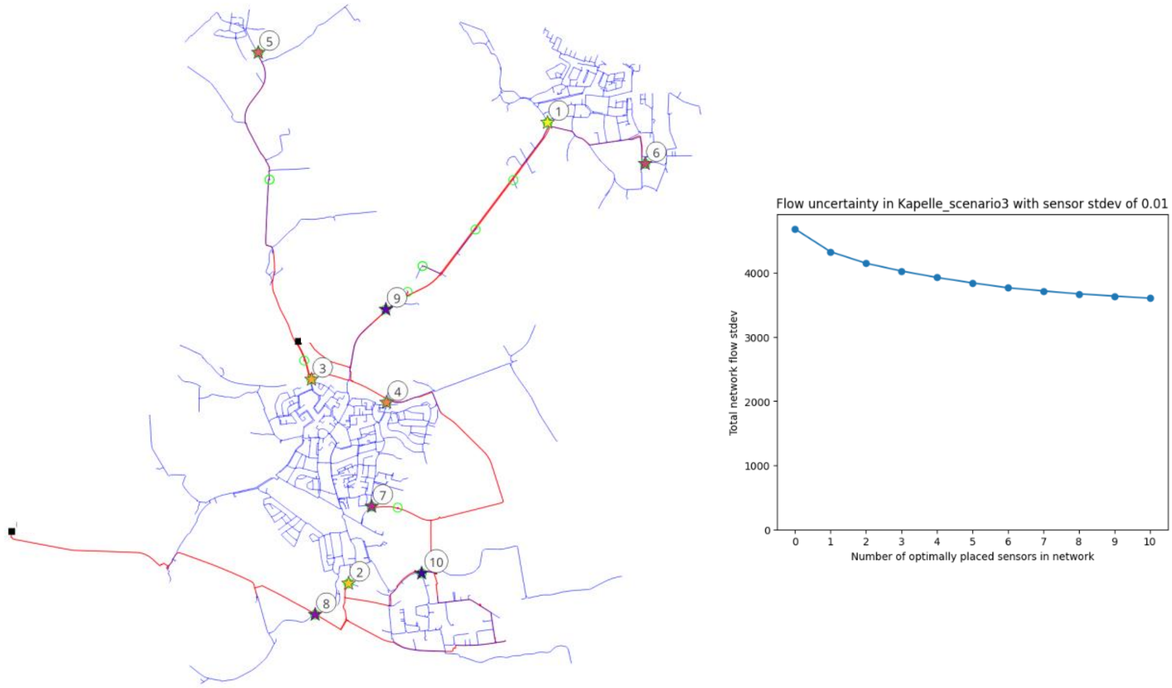


*Figure 4-29: Optimal flow sensor placement of 10 sensors for scenario 0, in the network of Kapelle (left). The coloured stars show the locations of the sensors and the green circles indicate the possible sensor locations, which are the locations of the stations. Reduction of total flow uncertainty as a function of the number of optimally placed sensors (right).*

The results for flow sensor placement for scenario 3 are illustrated in Figure 4-29. By comparing the results to scenario 0, the optimal sensor placement for the sensors 1, 2, 3 and 4 is the same. Sensor 1 is located in the North-East branch, sensor 2 is located near the industrial area South of Kapelle and sensor 3 near the gas supplier 1. The curve which shows the total flow uncertainty is also similar to the curve for scenario 0.

## 4.4 Findings

From the comparison of the results, a number of observations were made for the base scenario and scenario 1, 2, 3. For the pressure sensor placement, the optimal sensor locations were different for every scenario. Below the sensor locations are listed in a table, based on the station ID.

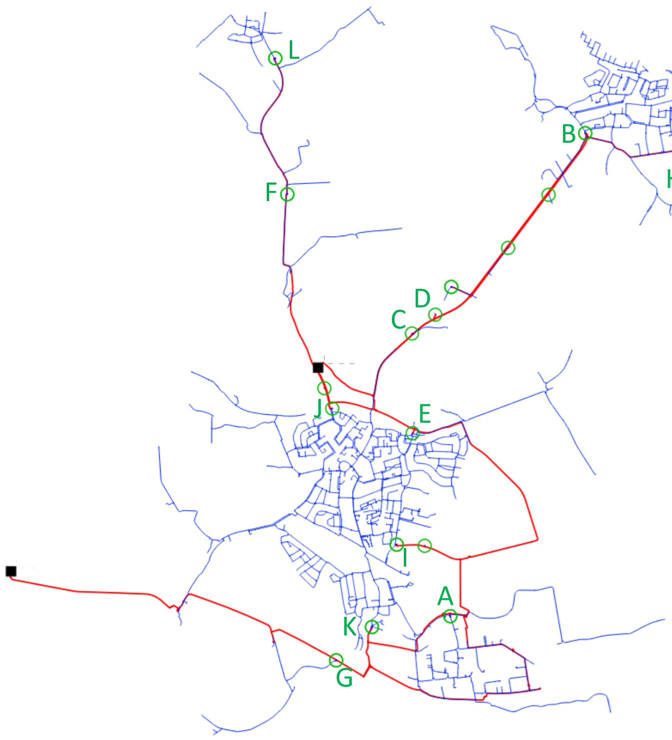


*Figure 4-30: Station IDs for the comparison of sensor placement.*

*Table 4-2: Comparison of optimal pressure sensor placement of 10 sensors for scenarios 0, 1, 2 and 3.*

| **Pressure sensor placement** | | | | |
|---|---|---|---|---|
| **# of sensor** | **Station ID** | | | |
| | **Scenario 0** | **Scenario 1** | **Scenario 2** | **Scenario 3** |
| **1** | A | A | A | A |
| **2** | B | B | B | B |
| **3** | C | C | J | L |
| **4** | D | D | C | F |
| **5** | E | E | D | C |
| **6** | F | G | F | E |
| **7** | G | F | G | D |
| **8** | H | I | E | G |
| **9** | I | H | H | I |
| **10** | J | J | L | J |

On Table 4-2, the optimal pressure sensor locations are listed for each scenario. The locations for the pressure sensors show some similarities and a few differences. Stations A and B are the first two choices for placing a pressure sensor, for all scenarios. Station A is located next to the industrial area, where a number of large consumers are in place whereas B is in the North-East area of Wemeldinge. Station C is chosen for the 3$^{rd}$ sensor for scenarios 0 and 1, and it is in located on the pipe that supplies Wemeldinge. For scenarios 2 and 3 the 3$^{rd}$ sensor is placed in stations J and L respectively. Station J is near the gas supplier 1 and it supplies with hydrogen the centre of Kapelle where the most of the small consumers are located. For scenario 2 the 4 bar pipe which connects gas supplier 1 and gas supplier 2 is removed, thus the mean flow rate through station J is increased. Station L is located in the area of Kattendijke, which is at a distance from Kapelle and it is supplied via a long 4 bar pipeline.

*Table 4-3: Comparison of optimal flow sensor placement for scenarios 0, 1, 2 and 3.*

**Flow sensor placement**

| # of sensor | Station ID | | | |
|---|---|---|---|---|
| | **Scenario 0** | **Scenario 1** | **Scenario 2** | **Scenario 3** |
| **1** | B | B | B | B |
| **2** | K | K | K | K |
| **3** | J | J | E | J |
| **4** | E | E | J | E |
| **5** | H | L | L | L |
| **6** | L | H | I | H |
| **7** | G | I | H | I |
| **8** | I | G | G | G |
| **9** | A | A | C | C |
| **10** | C | C | A | A |

On Table 4-3, the optimal flow sensor locations are listed for each scenario. The optimization algorithm suggests that for all four scenarios the first two sensors should be at stations B and K. Station B is located in the area of Wemeldinge and station K is located near the industrial area of Kapelle, in the South of the network. For the 3rd sensor, station J is chosen for scenarios 0, 1 and 3, which is next to gas supplier 1 and it supplies the center of Kapelle with hydrogen. For scenario 2, the 3rd sensor is placed at station E, which is located on the North side of the center of Kapelle, next to the disconnected pipeline. By disconnecting this pipe, the mean flow rate through station E is increased.

# 5 Discussion and Conclusion

The digitalization for future gas grid are divided into three categories: monitoring, modeling, and control. This report describes the use case of "smart sensor placement" to find optimal location for placing sensor for monitoring. However due to cost and timeline constraints, it is not possible to place sensors in all locations. Thus a combination of sensors and simulation models give a complementary insight for monitoring of gas grid.

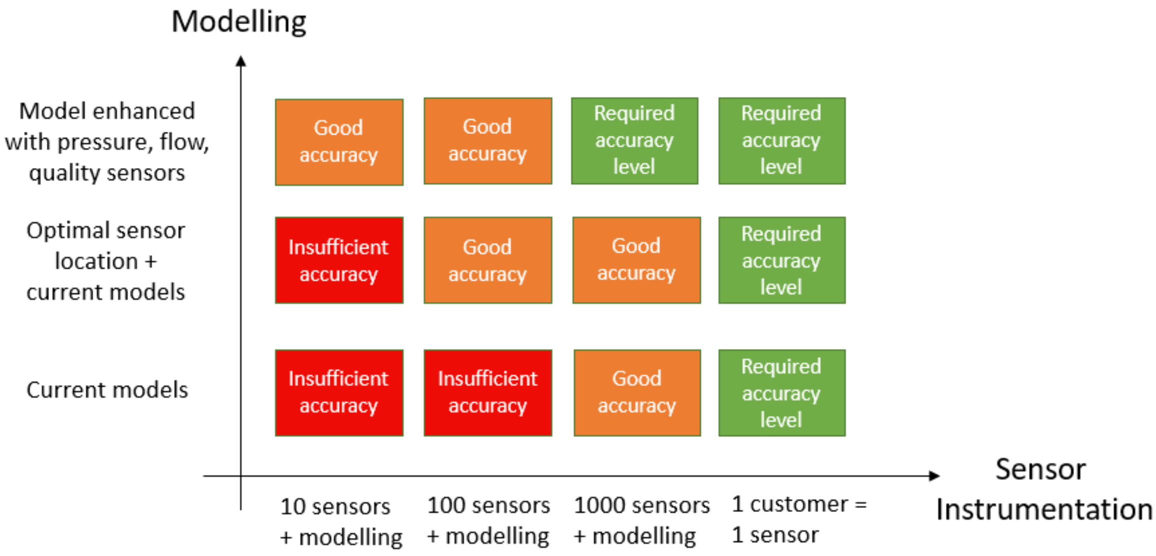


*Figure 5-1 Combination of simulation model and sensor instrumentation to increase accuracy*

Figure 5-1 shows that in order to have the required accuracy level, we need to install sensor in each consumer. With decreasing the number of sensors that are implemented in the network, the less information that you can get from the grid. In the current situation for DSO's, the pressure sensor is only available in some critical stations. There is no flow sensor implemented in the grid, only at the gas supplier 1 and at biogas feeders. Even though the penetration of smart meter implementation in each small consumer is high, the DSO currently does not have access to this smart meter. DSO's have only access to large consumer hourly flow data with a connection above 170 $m^3/h$. However it is still under discussion whether DSO can use randomised data which is privacy safe.

The next approach is using a digital model (or a gas grid simulator) to calculate pressure, flow and composition in the network. However this simulator is heavily depending on input data such as flow boundary condition of each consumer. Since we don't have access to the hourly consumption data, thus we need to have a consumer model that can calculate the hourly consumption data based on weather measurement, NEDU profiles and SJV value. Thus it can capture temporal dynamics from weather dependent profiles and also amplitude from the SJV value. The other parameters are the geometrical information from the system (e.g. pipe material, roughness, diameter, length, etc.). This parameters contribute in the pressure drop calculation in the system. Especially for a grid that has a lot of branches and ring topology, the pressure field will contribute to the flow direction in the network. Thus validation of the gas grid simulator model is needed to quantify the accuracy of the model w.r.t to measurement data.

The ideal situation would be to have all boundary input data that is coming from flow sensors in each consumer. In that case the simulation model will calculate the flow distribution in the network. And also by comparing pressure distribution in the network calculated by the model to pressure sensors in each station and consumer. When there is a mismatch between simulation and measurement, the model parameters can be tuned in order to improve the accuracy to the required level. However, in reality we don't have this luxury. Thus a limited number of sensors in optimal locations with combination of a validated simulator (tuned model) also can be used to have the required accuracy level.

As presented in section 2.1.4, we start validation our Aurora gas grid simulator with Kapelle network data. The pressure and flow calculation results for period of five weeks at the end of 2021 give a good match both in terms of the temporal profile and the amplitude. The mean percentage error of pressure calculation and available pressure measurement is 0.7%, while the mean percentage error of calculated flow and measured flow at gas supplier 1 is 8.81%. The accuracy of flow prediction is quite good enough remembering we don't have real-time measured small consumer flow data. This small consumer flow data is constructed based on a consumer model utilizing weather profile, NEDU profile and SJV. We do have real-time measurement data of 5 out of 17 large consumers flow profile which contribute 30-40% of total the flow during the work week and 5-10% of total flow during the weekend. Thus the uncertainty coming from flow profile is still high.

Since placing sensor in all locations is not realistic in the short term, then the "smart sensor placement" algorithm can help to determine optimal location for placing the pressure and flow sensor to reduce the uncertainties. The current workflow is that the network operator determines the location where to put the sensor based on operational requirements (e.g. station with long history of high pressure drops and outages or station with large capacity). As discussed in section 4.2, the algorithm shows that you only need two pressure sensors at the DS station to have a big reduction in the uncertainties of pressure. The third sensor onwards at DS station only improves a bit the standard deviation. If we zoom into the details, the algorithm finds the station with large pressure drop from the gas supplier 1 or gas supplier 2 as the main priority which is in line with the operational requirements. Without "smart sensor placement", the operator will have difficulty choose the priority to place the sensor because there are >5 stations within operational requirements criteria. For the flow sensor placement discussed in section 4.3, the improvement of placing flow sensors at DS station is not contributing a lot since the most uncertainties are close to small consumers on the street level. Due to the restriction of where to place the sensor (only at DS station), thus "smart sensor placement" is not showing their strong benefit, even though it gives priority insight where to put the flow sensor.

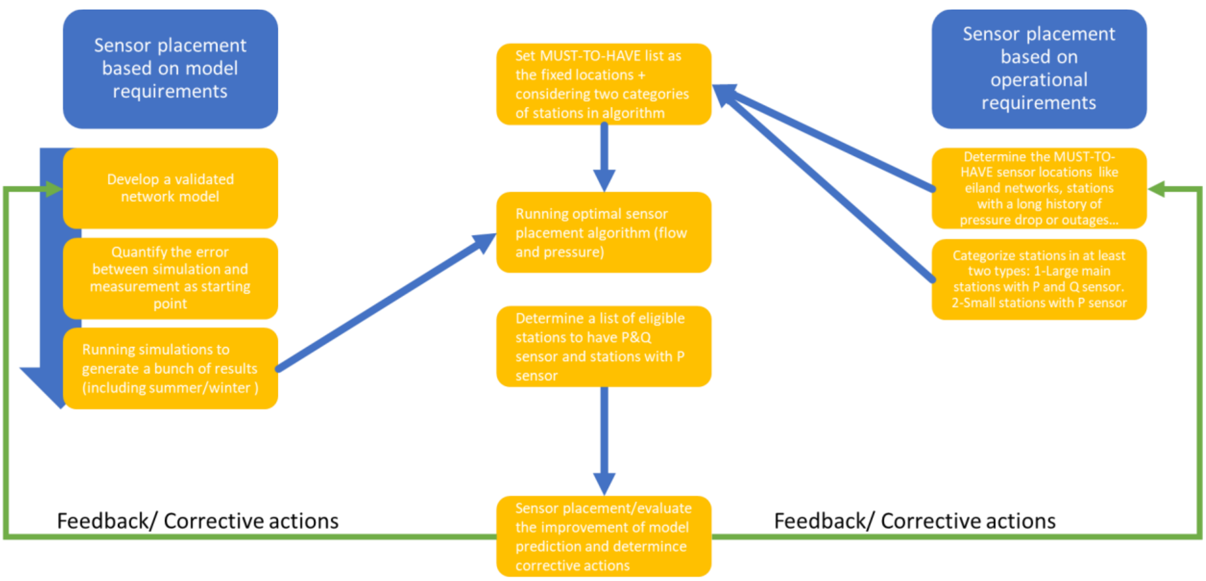

Figure 5-2 Proposed flowchart for sensor placement procedure

Since we have both the grid simulation model and “smart sensor placement” tool, we propose a flowchart to combine the sensor placement based on operational requirements. Figure 5-2 shows how these 2 approaches can work together. In the left side of the chart is the original workflow presented in this report. We start with developing a validated simulator model, quantify the error, running bunch of simulations results. Then before running “smart sensor placement”, the initial “Must Have” sensor location has been determined from the operational requirements as an input. Then the algorithm will give a list of where to place pressure and flow sensors. Once the sensor is implemented, we can use the real-time data to update the prediction from the simulation model. This procedure is then repeated as a feedback loop to determine the next sensor location.

# 6 Closing remarks on digitalization

In this chapter we give the results and conclusions on the key question of the whole research in WP8: What would be the need and benefit of digitalization in the future hydrogen grid?

We will answer this question in discussing the research questions (RQ's) as stated in the project plan.

1. How can digitalization contribute to an effective transition to hydrogen grids, maintaining security of supply?
2. How can digitalization contribute to a cost-effective decommissioning of the grid, maintaining security of supply?
3. What are the most interesting digitalization technologies to develop in the next 4 years to respond to the transition needs of DSOs?
4. Based on the available data from (previous) use cases:
    a. How will the demand profiles look? (Due to e.g., partly electrification, better insulation)
    b. How will the supply profiles be, due to local injection of hydrogen?
    c. What will the flows and pressures be in the grid and main assets?
    d. What measures in the grid should be taken to secure the supply of gas?
5. How will the trade-off be for the number of sensors and dedicated simulation tools?

The first three RQ's were investigated in the first half of the WP8 execution in performing the gap analysis between the current situation and the future hydrogen grid, on monitoring, modelling and control. At this moment the monitoring of the grid is very limited with flow measurement data at the gas supplier 1 and large consumer, and pressure measurement data at the gas supplier 1 and some rare (strategic) locations. In modelling the physical behavior of the grid, offline and static tools are used. Control of the grid is very limited. The stations are manually controlled.

The challenges of the future hydrogen grid where seen in:

1. Increasing dynamics in supply and demand, like changing user profiles, increasing decentralized supply and local storage and line-pack
2. From a stand-alone gas grid to a multi-connection grid. Observed trends are: connection to other DSO's, connection to Gasunie backbone and interaction with electricity grid (bi-directional)
3. Get access to real time data, on both Demand and Supply.

By extrapolating the current situation to the future, a roadmap of digitalization has been made describing the main technology developments in a timeline. On the short term real-time supply data should become available, together with more pressure measurements in the grid, to be used as input for a tool to simulate flow and pressure in an extended and complex grid. On the mid-term these technologies should be extended with flow and quality measurement in the grid (DS's), real time small consumer data and a more sophisticated tool to deal with dynamic profiles and transient effects in the network. The monitoring strategy can be supported by a tool that determines the number and locations of sensors in the grid. For the long-term there is a possible need for dealing with (local) storage and dynamic pressure management.

The topics of RQ4 and RQ5 has been answered in the second part of the WP8 execution, as described in the previous chapters of this report. Actually, in dealing with these RQ's we come to concrete argumentation in the need and benefit of digitalization.

Within the scope of this work, we didn't perform a detailed investigation on the demand profiles in case of hydrogen. In general more than 90% of the domestic gas consumption is for heating and hot water. For simplicity of the research we assumed that this will be the same for hydrogen. For sure the individual households will choose for other ways of heating, like (hybrid) heat pumps. This will have an effect on the individual consumptions and will lead to more uncertainty in demand. So that underlines the foreseen challenge in demand profiles for hydrogen grids and the need for more insight in the real-time behavior of the grid.

The supply profiles from electrolyzers connected to renewable sources have been used in the scenario's showing the effect of variable supply on the pressure and flow conditions in the grid. The dynamic added value of insight in the grid to prevent too high or too low pressures or too low flows to supply all customers at any time. Also in the grid design phase, is needed to choose the proper location of a supply.

The scenario on a pipe break and the effect on the flow and pressure distribution in the grid gives insight in how to deal with decommissioning of the grid, e.g. in case of decreasing (domestic) demand.

The different scenario's in this report show the need for a modelling tool that is able to calculate flows and pressures in the grid in case of a dynamic supply and demand situation, because of strong variable supply by e.g. wind turbines. But only a tool will not be sufficient to get full insight, because of uncertainties in the input data for the grid. In this report the effect of uncertainty in the demand profile has been studied. But one can think of other uncertainties, like incompleteness of the geometrical information (pipe diameters, pipe roughness, etc.) and pressure settings which deviate from the numbers that are used in the model.

So to get a full insight in the grid, always measurement data will be needed. The benefit of a simulation tool to investigate the number and location of sensors has been demonstrated. Especially the number of pressure sensors in the grid should be increased. To give a ball park figure, based on the Kapelle use case: with about 6000 domestic users and 20 industrial users one need two pressure sensors to reduce the uncertainty in pressure from 0.35 to 0.15 bar. So a reduction of about 60%. Also the preferred location of the sensor can be determined.

The benefit of using flow sensors is much smaller for this case. But it is preliminary to draw hard conclusions based on only one use case. The use of gas quality sensors has not been investigated, because this is seen as a more long-term topic. The gas quality criteria for hydrogen distribution grids are not yet defined, but one can foresee that with multiple hydrogen supply locations the quality in the grid will vary. On top of that the flows in the hydrogen grid are about three times higher than in the current natural gas situation. That means that contaminants in e.g. dead ends of the grid will be more pronounced.

Furthermore, the insight in the physical behavior of the grid is essential in the future foreseen increase of the number of decentralized hydrogen suppliers (both from solar/wind and surplus of the electricity grid) and the ability of DSO's to control or manage the pressure in the distribution network. The grid capacity management requirement will be different from the current green gas supply situation, as with the green gas we know production will be normally constant and the demand bottleneck will be mostly during the summer. So by reducing the pressure setting one time in the beginning of summer and increasing it in the beginning of the cold period, this can be solved in most cases. But with hydrogen this will be different, since we will have more players like hybrid heat pumps and congestion in electricity grid which may cause the need to create capacity by pressure management even in the winter to convert surplus electricity to hydrogen during the day and consuming it during night in hybrid heat pumps locally.

Overall, we can draw the conclusion on the added value of digitalisation of the gas grid. The gas grid is currently facing several broad challenges which can be aided by digital technologies: different heating technologies, declining amount of customers and gas demand, converting of the grid to hydrogen (and biomethane) and decentralised production. Current standard operations such as maintenance planning and security of supply can benefit from digitalisation, by allowing the DSO's to make better decisions and proper investments. Digitalisation will create more accurate and real-time insight and a combination of a robust calculation model and online data from a limited number of sensors will generate sufficient insight, moreover digitalisation will facilitate scenario analysis and creates more opportunities for renewable gasses in the gas network.

# 7 References

[1] R. Octaviano, H. Blokland and R. van der Linden, "D8.1 & D8.2 State of the art technologies in the current gas grid and gap definition with the future hydrogen grid," Zenodo, 2023.

[2] R. van der Linden, R. Octaviano, H. Blokland and T. Busking, "Security of Supply in Gas and Hybrid Energy Networks," *Energies,* vol. 4, no. 14, p. 792, 2021.

[3] I. A. Gondal and M. H. Sahir, "Prospects of natural gas pipeline infrastructure in hydrogen transportation," *International Journal of Energy Research,* vol. 36, no. 15, pp. 1338-1345, 2011.

[4] W. van Westering and H. Hellendoorn, "Optimal sensor placement using gas distribution network models: A case study," in *Proceedings of 2015 IEEE 12th International Conference on Networking, Sensing and Control*, Taipei, 2015.

[5] N. González Díez, L. van Lier, S. Belfroid and I. Meijer, "D1E.1 Impact of high speed hydrogen flow on system integrity and noise," Zenodo, 2022.

# 8 Appendix

## 8.1 Optimal pressure sensor placement – Impact on pressure uncertainty

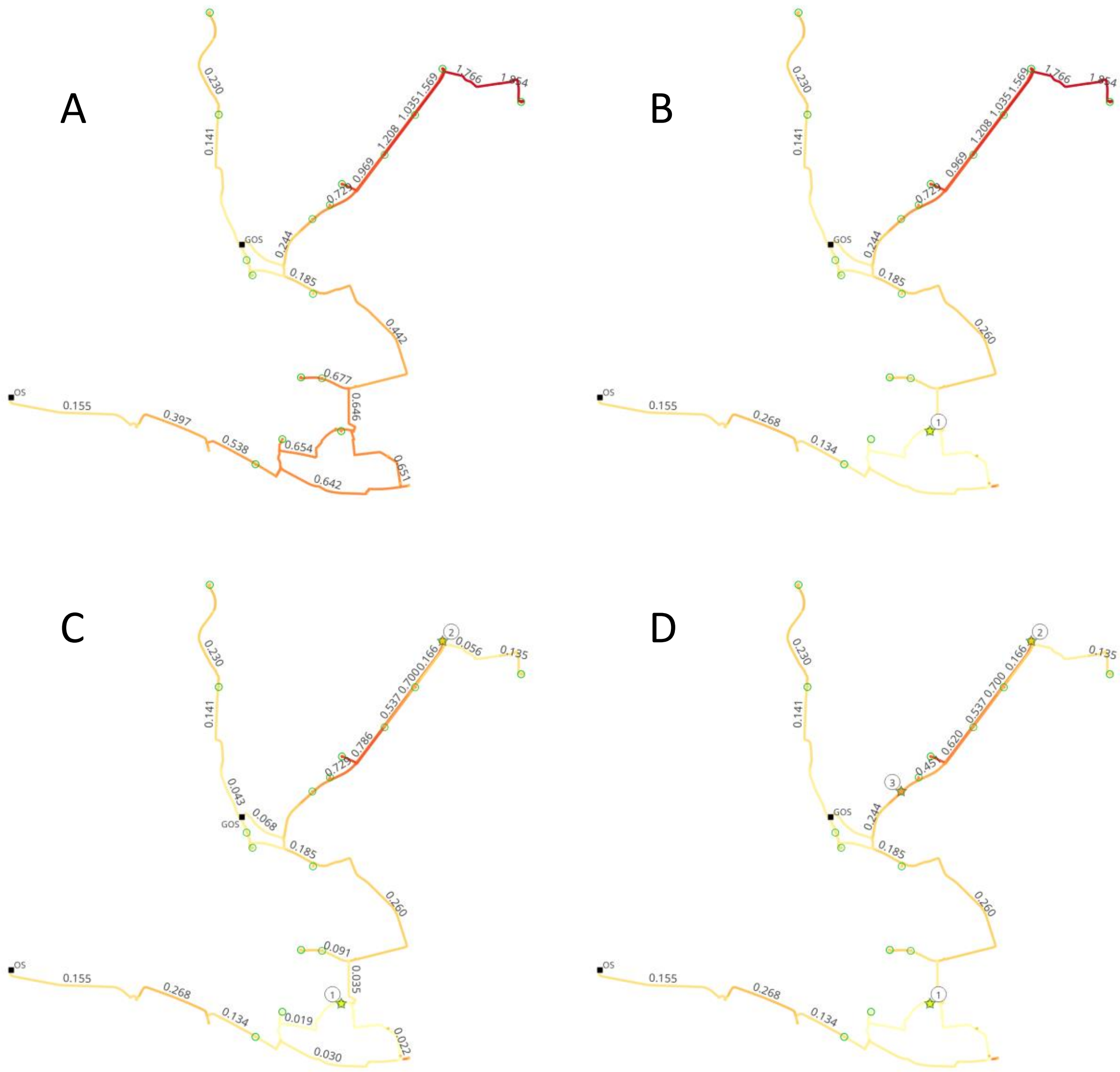


*Figure 8-1: Scenario 0, illustration of the impact of optimal pressure sensor placement on uncertainty. Subfigure **A** shows the pressure uncertainty without any sensors, **B** with 1 sensor, **C** with 2 sensors and **D** with 3 sensors. The units in all of the subfigures are in mbar.*

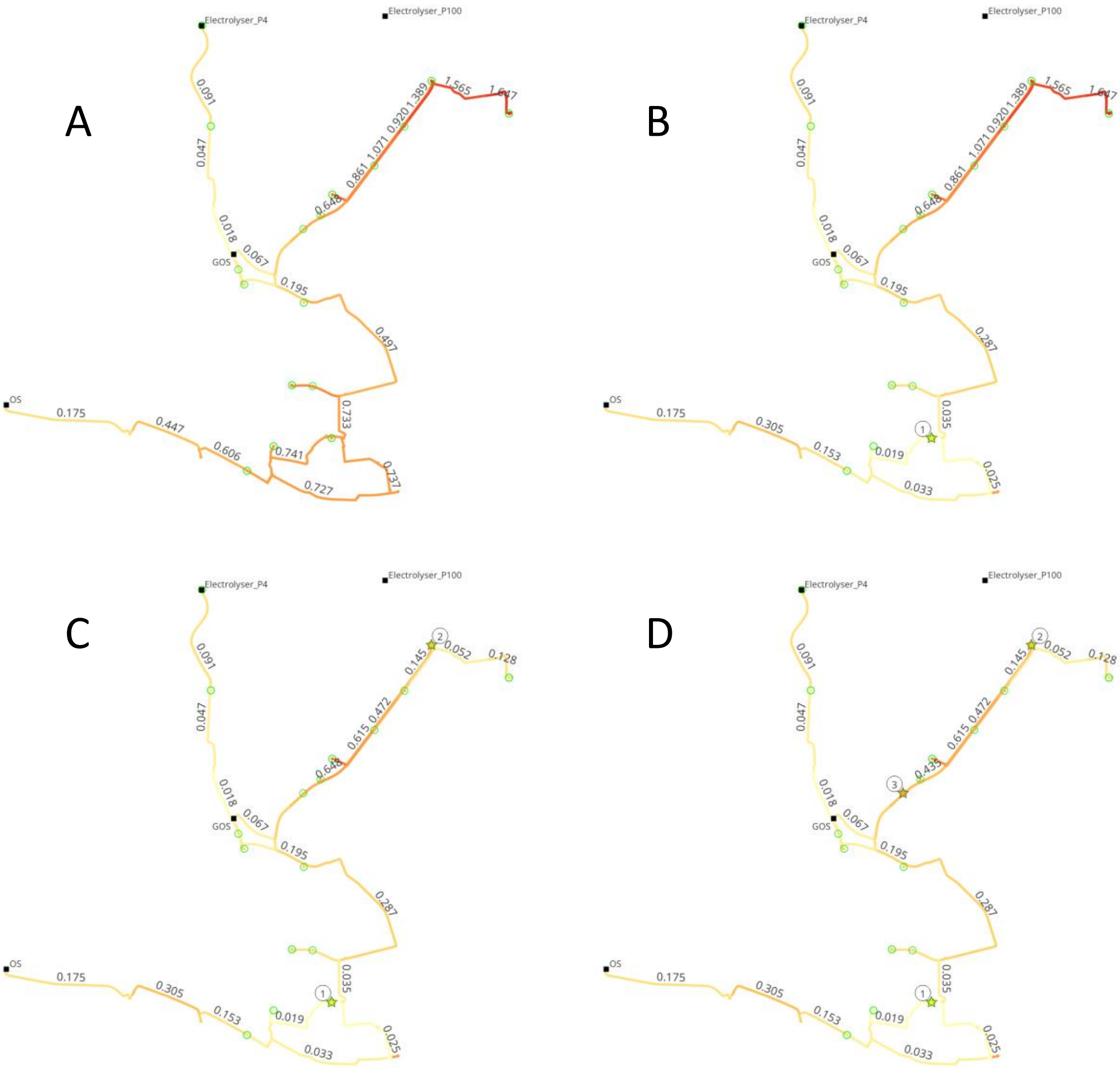


*Figure 8-2: Scenario 1, illustration of the impact of optimal pressure sensor placement on uncertainty. Subfigure **A** shows the pressure uncertainty without any sensors, **B** with 1 sensor, **C** with 2 sensors and **D** with 3 sensors. The units in all of the subfigures are in mbar.*

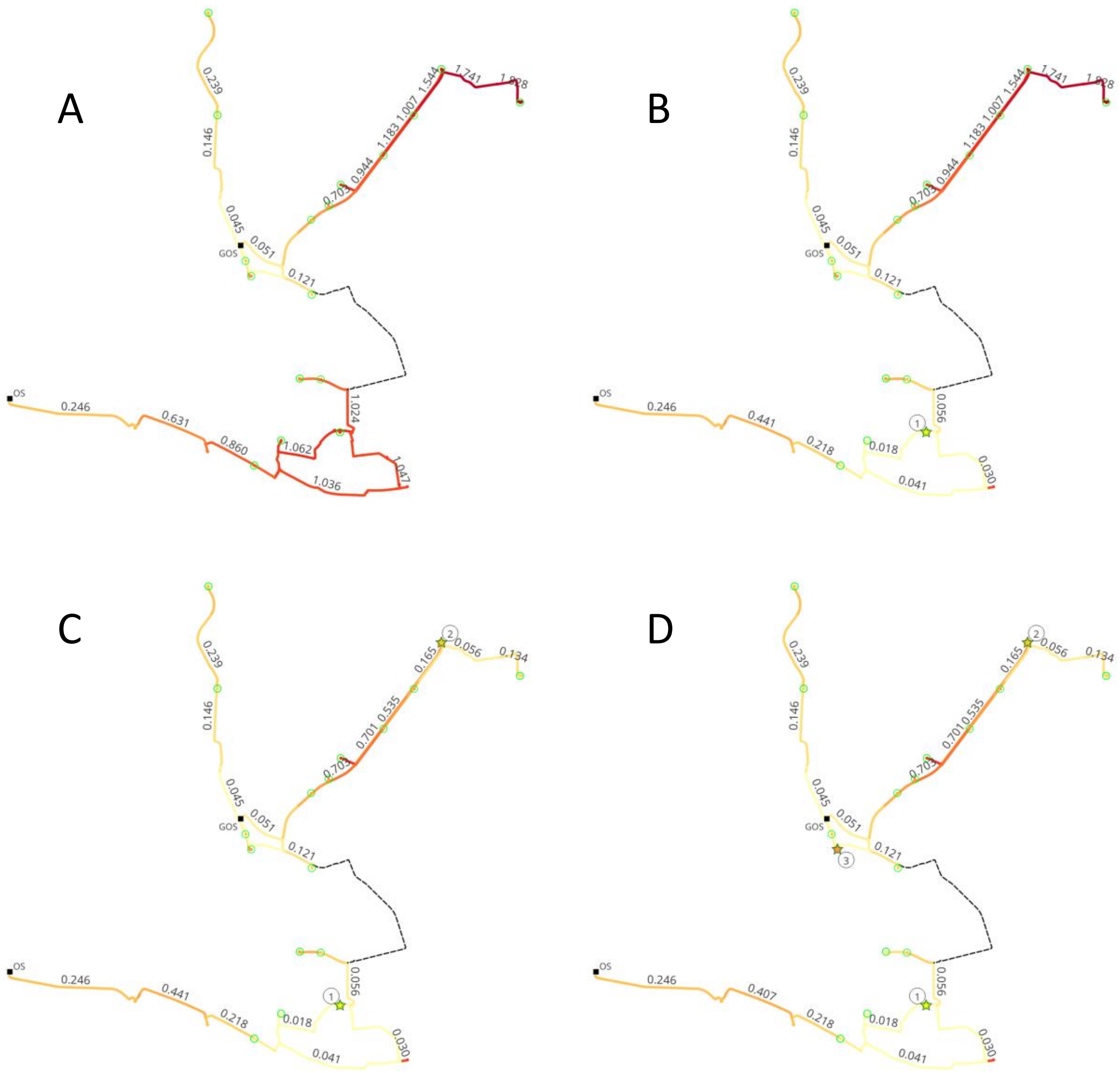


*Figure 8-3: Scenario 2, illustration of the impact of optimal pressure sensor placement on uncertainty. Subfigure **A** shows the pressure uncertainty without any sensors, **B** with 1 sensor, **C** with 2 sensors and **D** with 3 sensors. The units in all of the subfigures are in mbar.*

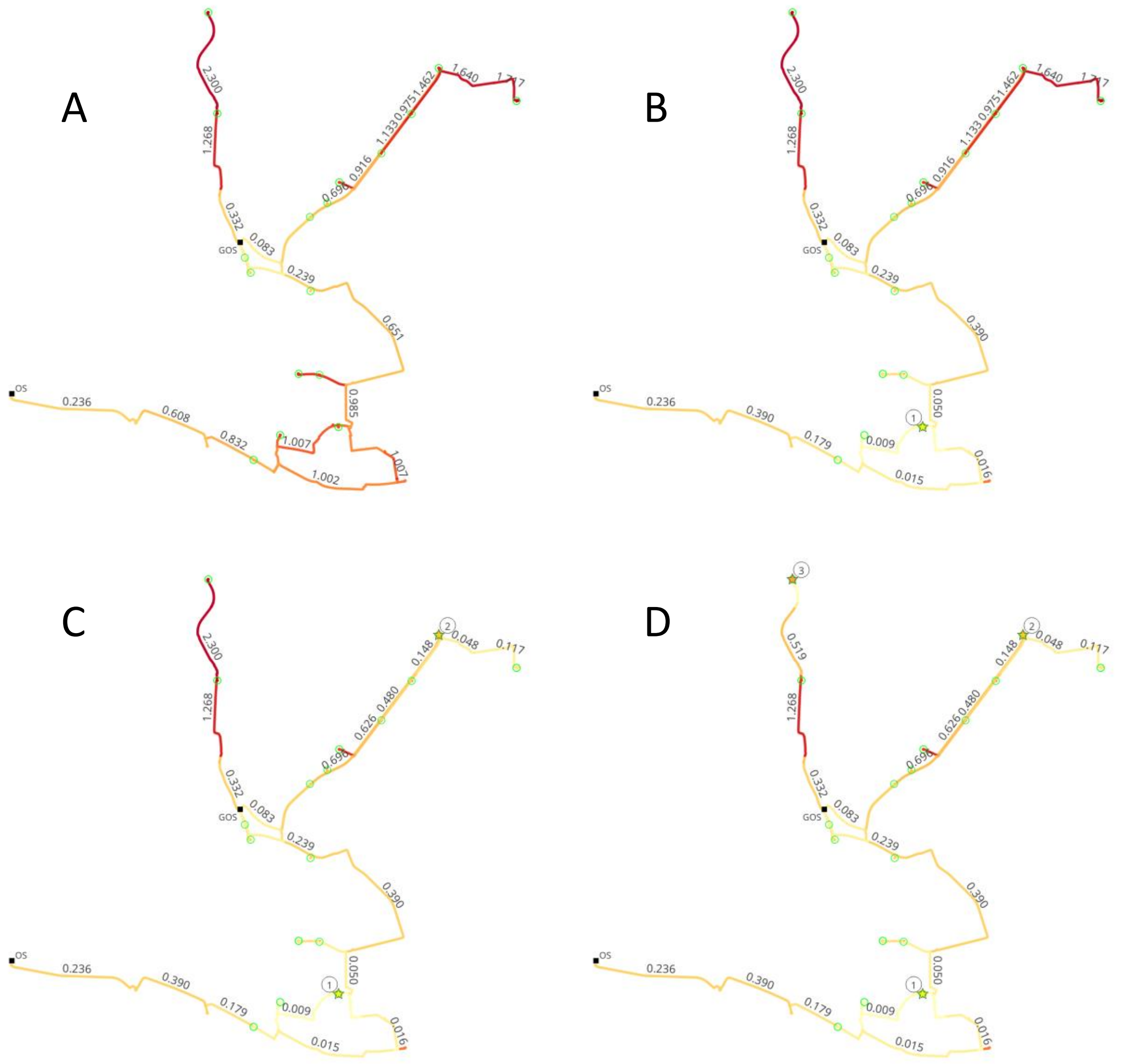


*Figure 8-4: Scenario 3, illustration of the impact of optimal pressure sensor placement on uncertainty. Subfigure **A** shows the pressure uncertainty without any sensors, **B** with 1 sensor, **C** with 2 sensors and **D** with 3 sensors. The units in all of the subfigures are in mbar.*

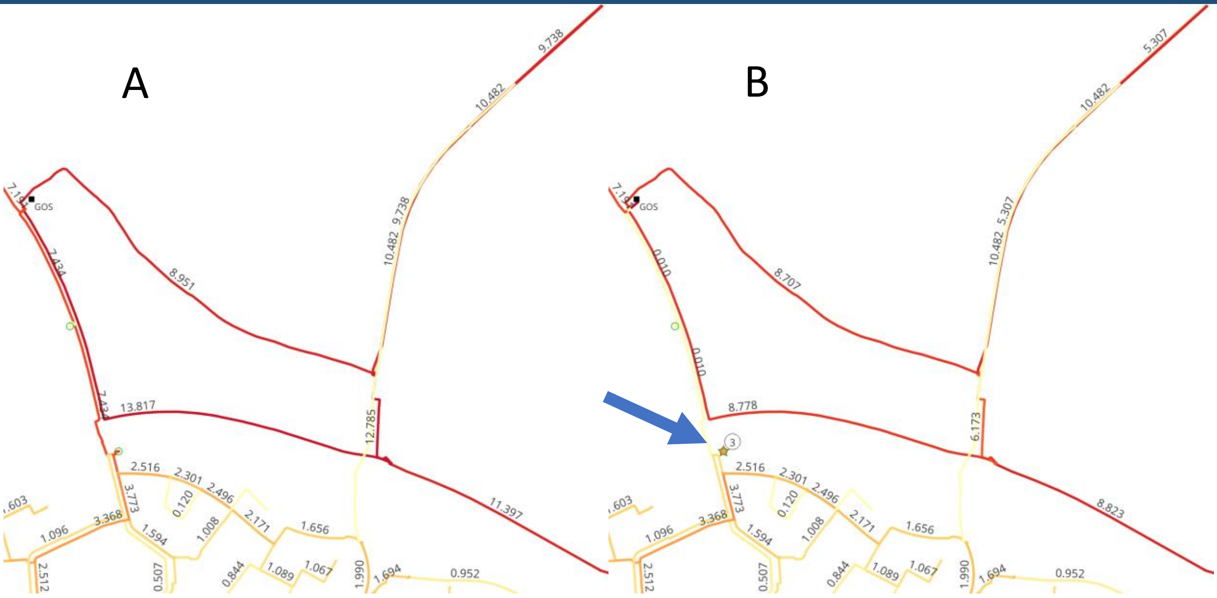


*Figure 8-5: The effect of the 3rd flow sensor on uncertainty in the nearby area, for scenario 0.*

## 8.2 Optimal flow sensor placement – Impact on flow uncertainty

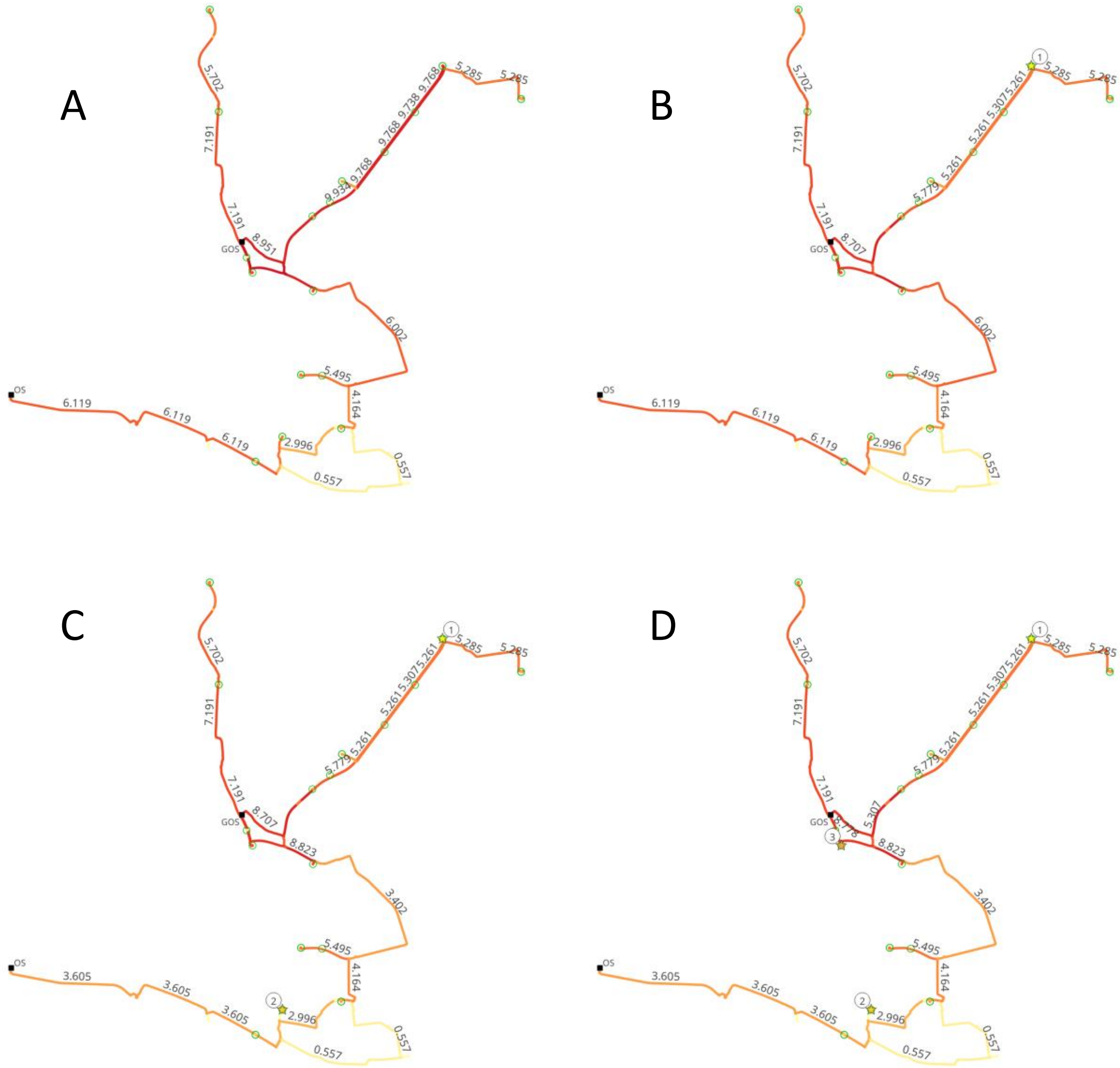


*Figure 8-6: Scenario 0, illustration of the impact of optimal flow sensor placement on uncertainty. Subfigure **A** shows the flow uncertainty without any sensors, **B** with 1 sensor, **C** with 2 sensors and **D** with 3 sensors. The units in all of the subfigures are in Nm³/hour.*

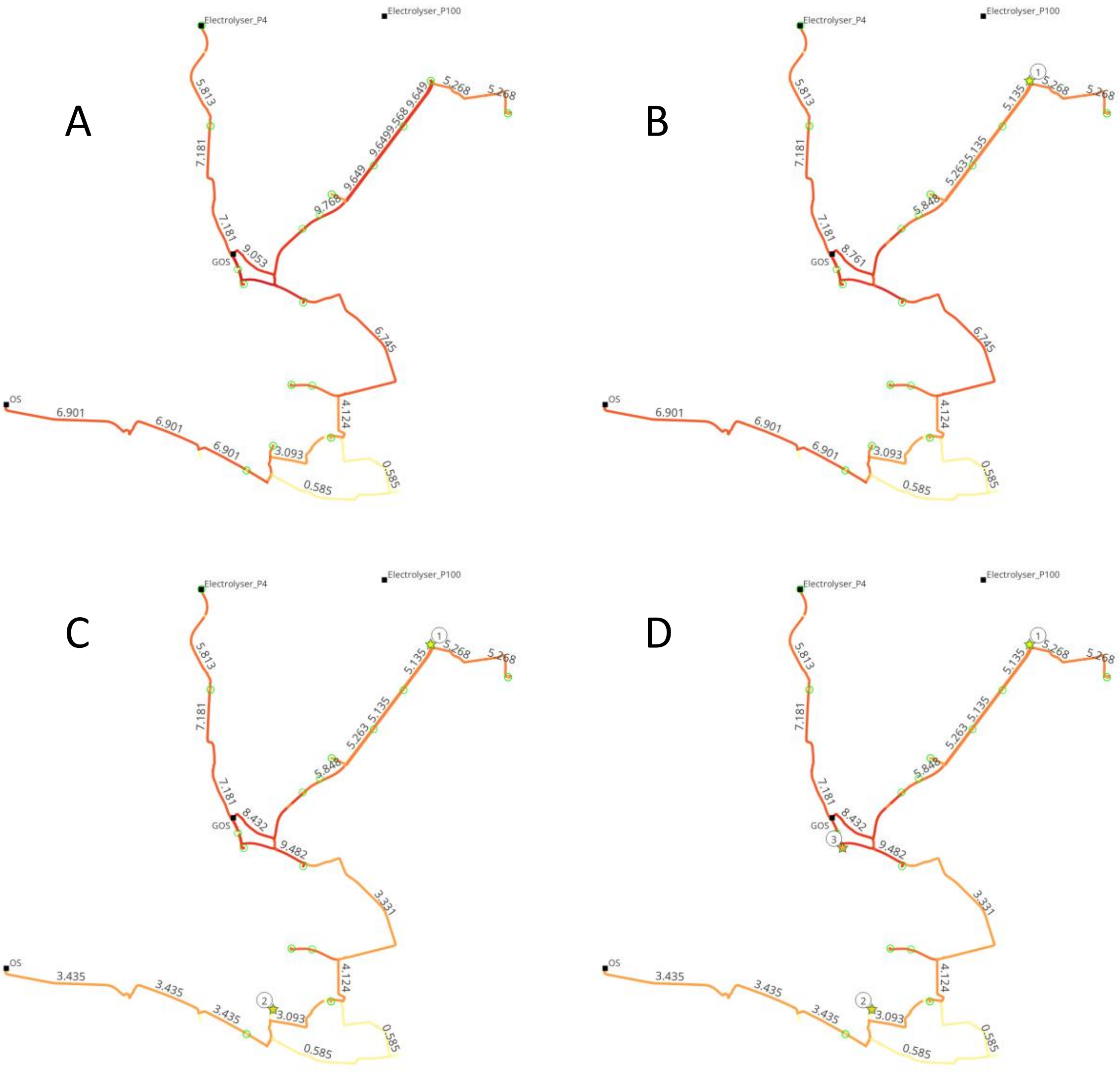


*Figure 8-7: Scenario 1, illustration of the impact of optimal flow sensor placement on uncertainty. Subfigure **A** shows the flow uncertainty without any sensors, **B** with 1 sensor, **C** with 2 sensors and **D** with 3 sensors. The units in all of the subfigures are in Nm$^3$/hour.*

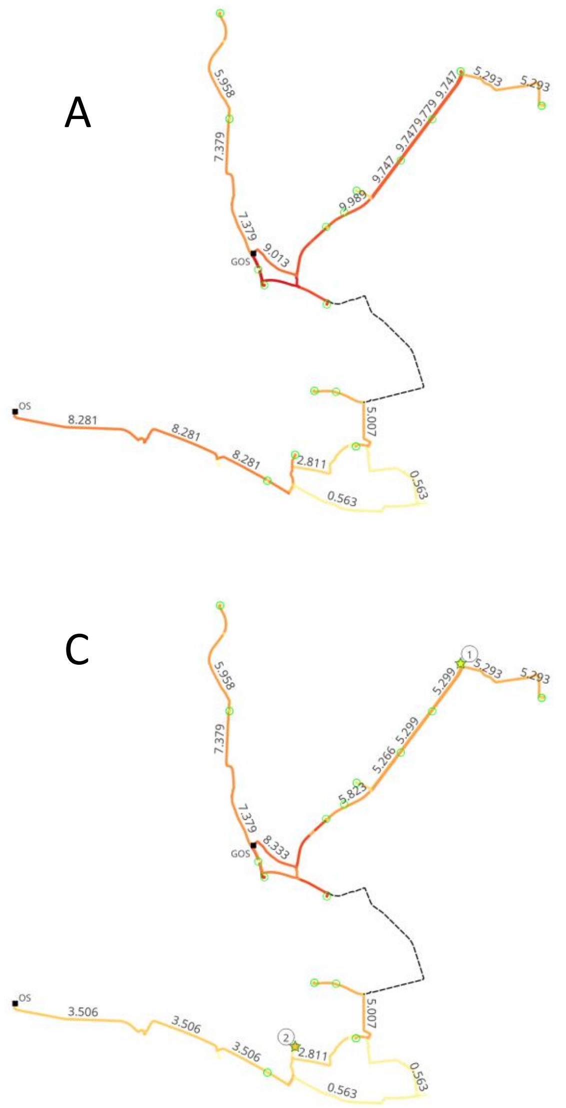


*Figure 8-8: Scenario 2, illustration of the impact of optimal flow sensor placement on uncertainty. Subfigure **A** shows the flow uncertainty without any sensors, **B** with 1 sensor, **C** with 2 sensors and **D** with 3 sensors. The units in all of the subfigures are in Nm³/hour.*

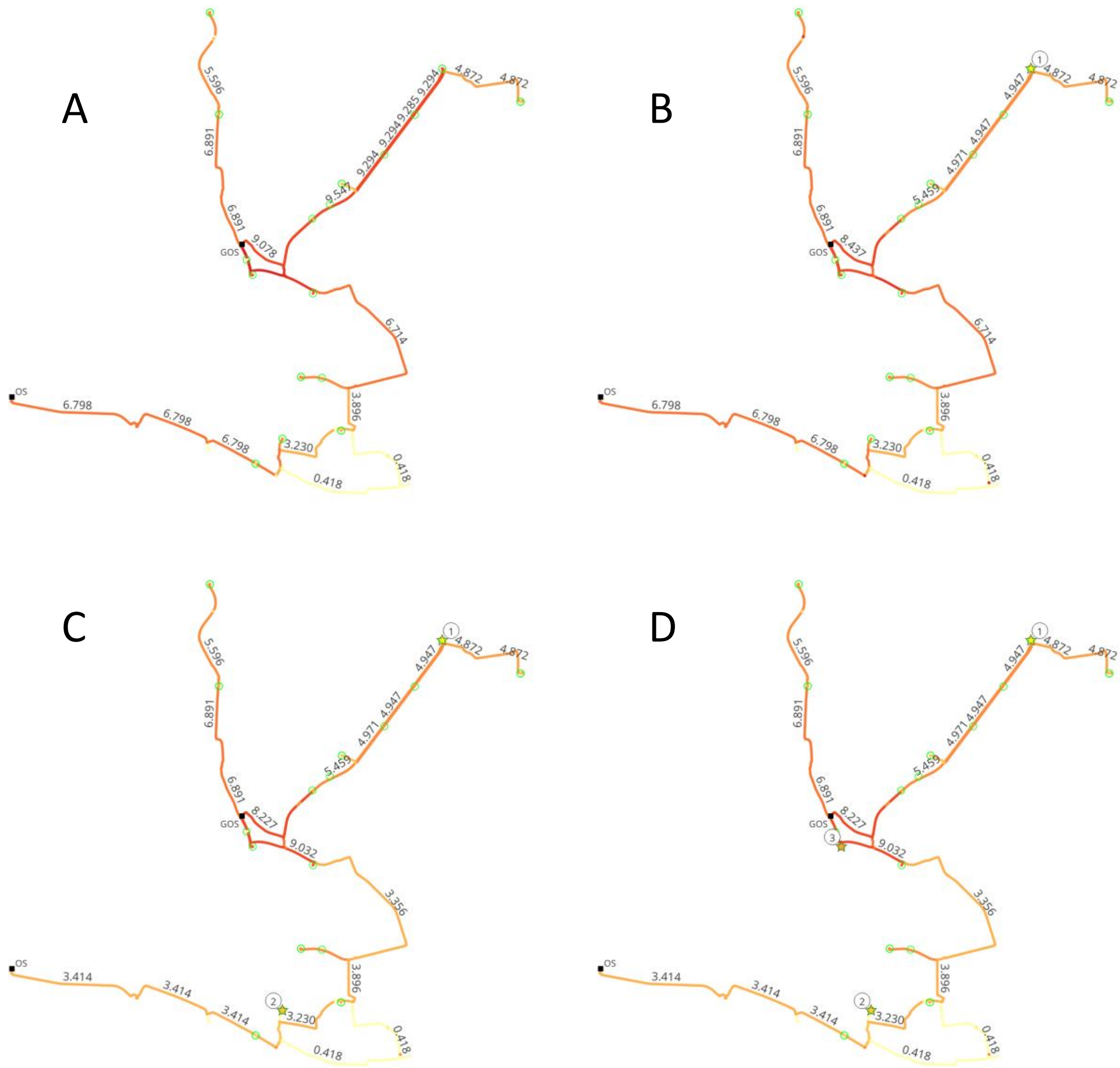


*Figure 8-9: Scenario 3, illustration of the impact of optimal flow sensor placement on uncertainty. Subfigure* ***A*** *shows the flow uncertainty without any sensors,* ***B*** *with 1 sensor,* ***C*** *with 2 sensors and* ***D*** *with 3 sensors. The units in all of the subfigures are in Nm³/hour.*